

RC
1042
.B87
1993

226680
M-491

D 7795 002



U.S. Department
of Transportation

**National Highway
Traffic Safety
Administration**

DOT HS 808 186

August 1993

Final Report

Evaluation of a Prototype Magnetohydrodynamic Angular Acceleration Transducer

This publication is distributed by the U.S. Department of Transportation, National Highway Traffic Safety Administration, in the interest of information exchange. The opinions, findings and conclusions expressed in this publication are those of the author(s) and not necessarily those of the Department of Transportation or the National Highway Traffic Safety Administration. The United States Government assumes no liability for its contents or use thereof. If trade or manufacturers' name or products are mentioned, it is because they are considered essential to the object of the publication and should not be construed as an endorsement. The United States Government does not endorse products or manufacturers.

1. Report No. DOT HS 808 186		2. Government Accession No.		3. Recipient's Catalog No.	
4. Title and Subtitle Evaluation of a Prototype Magnetohydrodynamic Angular Acceleration Transducer				5. Report Date August 1993	
				6. Performing Organization Code	
				8. Performing Organization Report No. VRTC-82-0226	
7. Author(s) W. Vincent Burke				10. Work Unit No. (TRAIS)	
9. Performing Organization Name and Address National Highway Traffic Safety Administration Vehicle Research and Test Center P.O. Box 37 East Liberty, Ohio 43319				11. Contract or Grant No.	
				13. Type of Report and Period Covered Final Report	
12. Sponsoring Agency Name and Address National Highway Traffic Safety Administration 400 Seventh Street, S.W. Washington, D.C. 20590				14. Sponsoring Agency Code	
15. Supplementary Notes					
16. Abstract In 1989, Applied Technology Associates, Inc. (ATA) reported the development of a magnetohydrodynamic (MHD) angular velocity sensor. Initial response to this sensor was positive, although users encountered difficulties when digitally differentiating the signal to angular acceleration. ATA then developed the model AAS-01 angular acceleration transducer, incorporating on-board analog differentiation circuitry with the angular velocity sensing element. An evaluation of a prototype AAS-01 is presented in this document. The performance of this new transducer was assessed in a variety of dummy head test environments, including: head/neck pendulum, direct linear impacts, and free-motion impacts into an automotive windshield. A Hybrid III dummy head was instrumented with three of the MHD angular acceleration transducers, an MHD angular velocity sensor, and the 3-2-2-2 linear accelerometer array commonly used for measurement of head angular acceleration The results of this study indicate that the MHD and 3-2-2-2 angular acceleration signals are quite comparable in low frequency test environments, but deviate under higher energy direct impacts. Frequency analysis revealed that SAE Class 600 (-3 Db at 1000 Hz) channels, at a minimum, are required to capture all significant data for determination of head angular acceleration. Finally, this report offers suggestions for improvement of the MHD instrumentation package and practical information for users of the angular motion sensors.					
17. Key Words			18. Distribution Statement Document is available to the public from the National Technical Information Service, Springfield, VA 22161		
19. Security Classif. (of this report) Unclassified	20. Security Classif. (of this page) Unclassified	21. No. of Pages 12	22. Price \$12.00		

METRIC CONVERSION FACTORS

Approximate Conversions to Metric Measures

Approximate Conversions from Metric Measures

When You Know			When You Know		
Symbol	Know	To Find	Symbol	Know	To Find
LENGTH			LENGTH		
in	inches	centimeters	mm	millimeters	inches
ft	feet	centimeters	cm	centimeters	inches
yd	yards	meters	m	meters	feet
mi	miles	kilometers	km	kilometers	yards
AREA			AREA		
in ²	square inches	square centimeters	cm ²	square centimeters	square inches
ft ²	square feet	square meters	m ²	square meters	square yards
yd ²	square yards	square meters	km ²	square kilometers	square miles
mi ²	square miles	square kilometers	he	hectares	acres
acres	acres	hectares	(10,000m ²)	(10,000m ²)	
MASS (weight)			MASS (weight)		
oz	ounces	grams	g	grams	ounces
lb	pounds	kilograms	kg	kilograms	pounds
(2000 lbs)	short tons	metric ton	t	metric ton	short tons
VOLUME			VOLUME		
tsp	teaspoons	milliliters	mL	milliliters	fluid ounces
Tbsp	tablespoons	milliliters	mL	milliliters	cubic inches
in ³	cubic inches	milliliters	L	liters	pints
fl oz	fluid ounces	milliliters	L	liters	quarts
c	cups	liters	m ³	cubic meters	gallons
pt	pints	liters	m ³	cubic meters	cubic feet
qt	quarts	liters			cubic yards
gal	gallons	liters			
ft ³	cubic feet	cubic meters			
yd ³	cubic yards	cubic meters			
TEMPERATURE			TEMPERATURE		
°F	degrees Fahrenheit	5/9 (after subtracting 32)	°C	degrees Celsius	9/5 (then add 32)

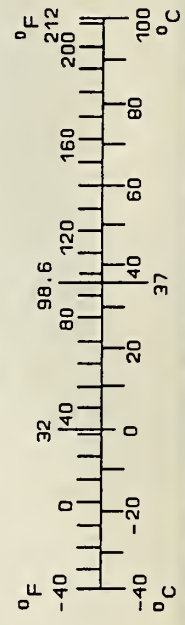


TABLE OF CONTENTS

	Page
TECHNICAL REPORT DOCUMENTATION PAGE	i
METRIC CONVERSION FACTORS	ii
LIST OF FIGURES	iv
LIST OF TABLES	v
TECHNICAL SUMMARY	vii
1.0 INTRODUCTION	1
2.0 TEST PROCEDURES	1
2.1 Power Supply Noise	3
2.2 Head/Neck Pendulum Testing	4
2.3 Linear Transfer Pendulum Impact Testing	4
2.4 Free-Motion Windshield Impacts	6
2.5 Data Handling	6
3.0 RESULTS	7
3.1 Power Supply Noise	7
3.2 Cross-Axis Sensitivity	7
3.3 Head/Neck Pendulum Testing	9
3.3.1 IETL-001 Comparisons to AAS-01 (Analog vs. Digital Differentiation)	13
3.4 Linear Transfer Pendulum Testing	13
3.5 Free-Motion Windshield Impacts	16
4.0 DISCUSSION	22
5.0 CONCLUSIONS	30
6.0 REFERENCES	31
APPENDIX A	33
APPENDIX B	37

LIST OF FIGURES

	Page
Figure 1 – Head Coordinate System	2
Figure 2 – Head Instrumentation Package	3
Figure 3 – Power Supply Noise Testing	4
Figure 4 – Head/Neck Pendulum Test	5
Figure 5 – Direct Impact (Frontal)	5
Figure 6 – Free-Motion Headform Projected into Windshield	6
Figure 7 – Power Spectra for Power Supply Noise Tests	8
Figure 8 – Head/Neck Pendulum Angular Accelerations	11
Figure 9 – Power Spectra from Pendulum Tests	12
Figure 10 – IETL-001 Angular Velocity Measurement and Differentiation	14
Figure 11 – AAS-01, 3-2-2-2, and Differentiated IETL-001 Ang Accels	15
Figure 12 – Low Speed Direct Impact Angular Accelerations	17
Figure 13 – High Speed Direct Impact Angular Accelerations	18
Figure 14 – Power Spectra for Low Speed Linear Impacts	19
Figure 15 – Power Spectra for High Speed Linear Impacts	20
Figure 16 – Ringing of Z-Axis AAS-01	21
Figure 17 – Angular Accelerations from Windshield Impacts	23
Figure 18 – Power Spectra for Windshield Impacts	24
Figure 19 – Narrow View of High Frequencies from Windshield Impacts	25
Figure B1 – Clipped Channel (Test 02260058)	
Figure B2 – Corrected Channel	

LIST OF TABLES

Page

TABLE 1 – Cross Axis Angular Error	9
TABLE 2 – Head/Neck Pendulum Testing Angular Accelerations AAS-01 vs. 3-2-2-2	10
TABLE 3 – IETL-001 vs. AAS-01	13
TABLE 4 – Direct Head Impacts	15
TABLE 5 – Filtering of AAS-01 Angular Acceleration	27
TABLE 6 – Filtering of 3-2-2-2 Angular Acceleration	28

**Department of Transportation
National Highway Traffic Safety Administration
TECHNICAL SUMMARY**

Report Title: Evaluation of a Prototype Magnetohydrodynamic Angular Acceleration Transducer	Date: August, 1993
Report Author(s): W. Vincent Burke	

In 1989, Applied Technology Associates, Inc. (ATA) reported the development of a magnetohydrodynamic angular velocity sensor. Initial response to this sensor was positive, although users encountered difficulties when digitally differentiating the signal to angular acceleration. ATA then developed the model AAS-01 angular acceleration transducer, incorporating on-board analog differentiation circuitry with the angular velocity sensing element. An evaluation of a prototype AAS-01 is presented in this document.

The performance of this new transducer was assessed in a variety of dummy head test environments, including: head/neck pendulum, direct linear impacts, and free-motion impacts into an automotive windshield. A Hybrid III dummy head was instrumented with three of the MHD angular acceleration transducers, an MHD angular velocity sensor, and the 3-2-2-2 linear accelerometer array commonly used for measurement of head angular acceleration

The results of this study indicate that the MHD and 3-2-2-2 angular acceleration signals are quite comparable in low frequency test environments, but deviate under higher energy direct impacts. The lack of a true reference angular acceleration prohibits determining which of the two systems is more accurate. Frequency analysis revealed that SAE Class 600 (-3 dB at 1000 Hz) channels, at a minimum, are required to capture all significant data for determination of head angular acceleration in common dummy test exposures. Finally, this report offers suggestions for improvement of the MHD instrumentation package and practical information for users of the angular motion sensors.

1.0 INTRODUCTION

In 1989, Applied Technology Associates, Inc. (ATA) reported development of an IETL-001 first generation magnetohydrodynamic (MHD) angular rate sensor¹. The sensor immediately found application and acceptance in automotive testing for the measurement of angular velocity and (by integration) angular displacement. The operating principle of the magnetohydrodynamic sensors has been described by Laughlin¹. Briefly, these sensors incorporate two magnets attached to a cylindrical housing. An annular column of mercury is held within the magnetic field. Upon rotation, an electrical potential is generated by the relative angular velocity difference between the conductive fluid and the applied magnetic field.

Early evaluations of the IETL-001 by both ATA¹ and the Naval Biodynamics Laboratory (NBDL)² revealed promising results. However, when used in high frequency test environments (e.g. direct linear impacts), the IETL-001 sensor has not been successful in providing a clean angular acceleration signal via mathematical differentiation of the angular velocity signal. The wide bandwidth of the instrument (-3 dB at 2,500 Hz), inherent sensor noise, differentiation techniques, and variability in signal conditioning electronics may all contribute to the problems encountered in differentiating the signal.

Feedback from users of the IETL-001 motivated ATA to create a second version of the MHD sensor specifically dedicated to angular acceleration. This new sensor, the AAS-01, provides direct output of angular acceleration by incorporating on-board analog differentiation circuitry to the angular velocity sensing element described above. The AAS-01 also uses an amplifier chip with markedly lower noise characteristics (-3 dB at 500 Hz) than that of the IETL-001. This study evaluates the AAS-01 sensor as a means of determining dummy head rotational acceleration in a variety of head impact test exposures.

2.0 TEST PROCEDURES

The first set of tests in this program were designed to look at the inherent noise and error characteristics of the AAS-01. Upon completion of the sensitivity testing, the AAS-01 sensors were placed in a Hybrid III dummy head and tested in common anthropomorphic test device (ATD) exposures. A Hybrid III head was instrumented with the 3-2-2-2 nine accelerometer array commonly used by the National Highway Traffic Safety Administration, three AAS-01's (one along each axis) and one IETL-001

(also aligned about the head y-axis). Figure 1 (modified from reference 3) illustrates the head coordinate system used for this study.

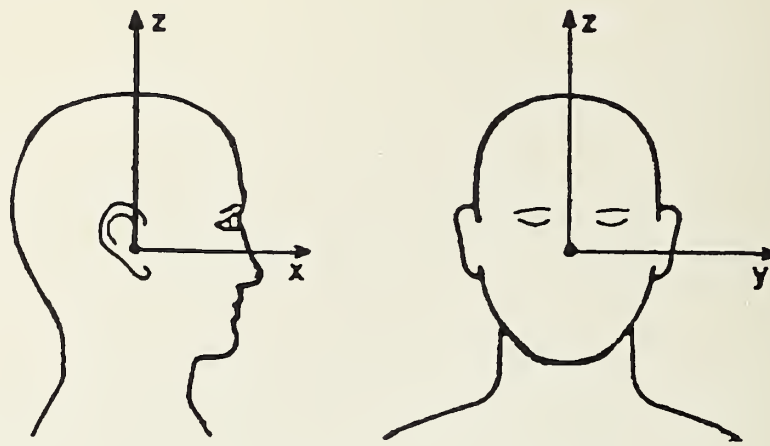


Figure 1 – Head Coordinate System

The 3-2-2-2 linear accelerometer array is mounted in a modified Hybrid III skull by placing three Endevco 7264/2000g accelerometers at the head center of gravity, and two accelerometers at the top, front, and left side of the dummy skull. The complete array allows angular acceleration to be calculated about each of the three head axes. Derivation of the equations to calculate angular accelerations is beyond the scope of this report and has been previously documented⁴.

A fixture was specially designed to allow mounting of the four MHD sensors in the skull while preserving the standard configuration of the 3-2-2-2 array. Each sensor was carefully installed so that the sensitive axis was orthogonal to the base of the inner skull. Assuming the dummy skull undergoes rigid-body motion, all points on the skull will experience identical rotational velocities and accelerations. It was therefore unnecessary for the sensitive axes of the rotational sensors to align with the head center of gravity. The changes in head cg and moment of inertias induced by the added sensor weight were not relevant to this study. Figure 2 illustrates the mounting of the head instrumentation.

CENTER, TOP AND FRONT MOUNTS
FOR 3-2-2-2 LINEAR ACCELEROMETER
ARRAY

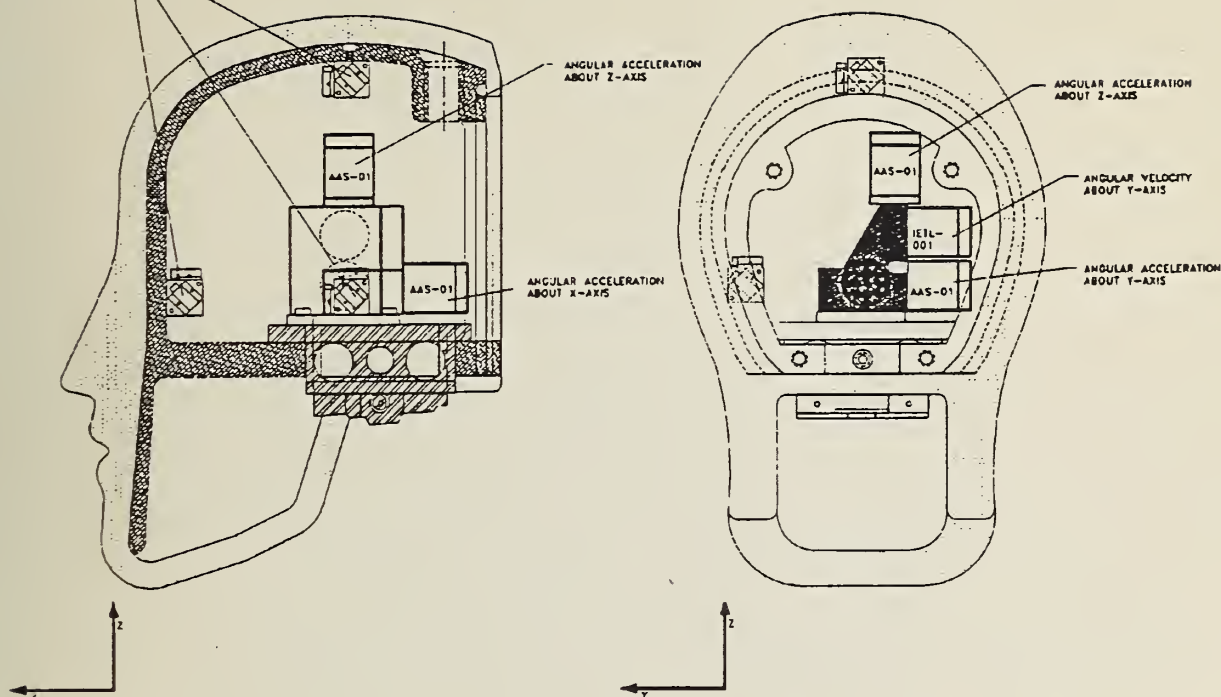


Figure 2 - Head Instrumentation Package

2.1 Power Supply Noise

The ATA MHD sensors operate using a bipolar ± 5 to ± 15 Volt DC excitation. Many data acquisition systems (including the Metraplex in place at the VRTC) provide unipolar DC excitation only, requiring that a separate power supply be built for the MHD sensors. To determine the amount of noise generated by the external power supply, an output signal was recorded with the sensor at rest. A vise clamped one IETL-001 and four AAS-01 sensors as shown in Figure 3, prohibiting any angular motion during data recording. Three separate power supplies were tested in this manner.

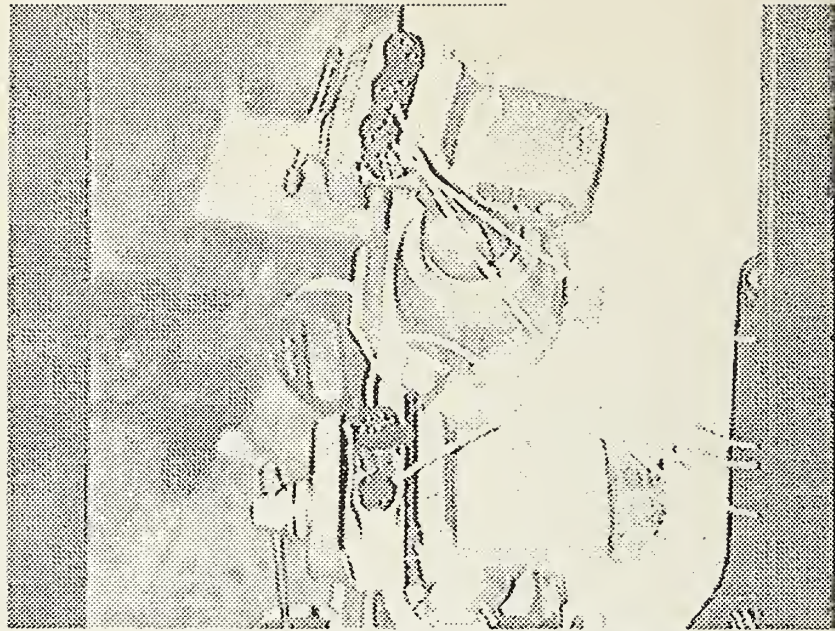


Figure 3 – Power Supply Noise Testing

2.2 Head/Neck Pendulum Testing

The Head/Neck pendulum provided a "soft", low frequency exposure with no external contacts to the head. This series of tests was conducted using the instrumentation scheme previously described: the 3-2-2-2 array, three AAS-01's, and one IETL-001. All testing was performed at the standard dummy certification velocity of 6.7 m/sec. The head was tested in three separate orientations: frontal (major rotation about head y-axis), lateral (rotation about the head x-axis), and oblique (15° offset about z-axis, providing multi-axis rotation). Three tests were performed in each of these configurations. Data from this test series were also used to study the cross-axis angular acceleration sensitivity of the respective measurement systems. Figure 4 shows a typical head/neck pendulum test.

2.3 Linear Transfer Pendulum Impact Testing

To illustrate the sensors' behavior in a higher frequency test environment, direct impacts were delivered to the head of a fully assembled, seated dummy. A 23.3 kg impact ram was fired at both 2.1 m/sec and 4.3 m/sec. Again, impacts were conducted in three different orientations: frontal, lateral, and oblique (35° offset about z-axis). Figure 5 displays a frontal impact.

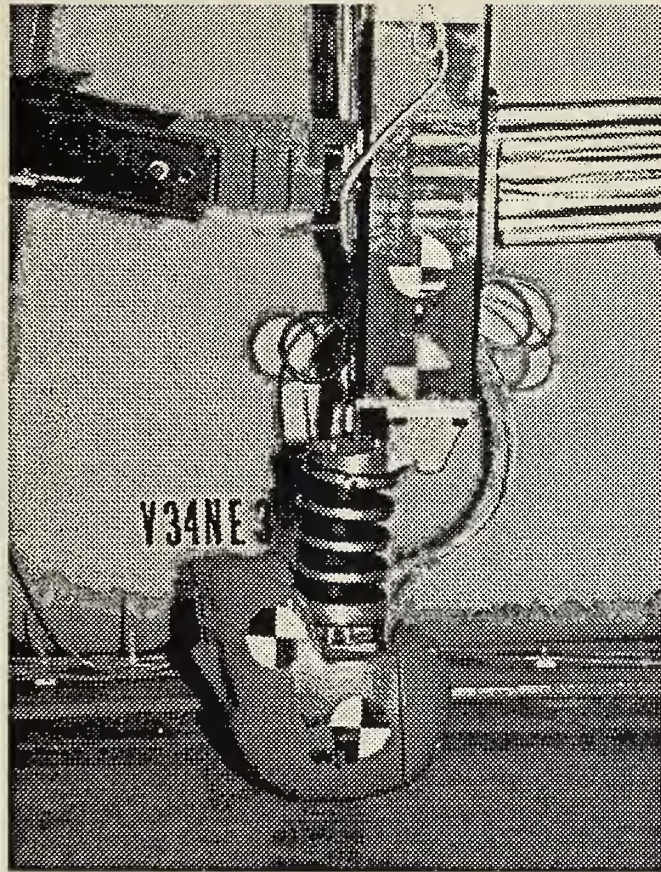


Figure 4 – Head/Neck Pendulum Test

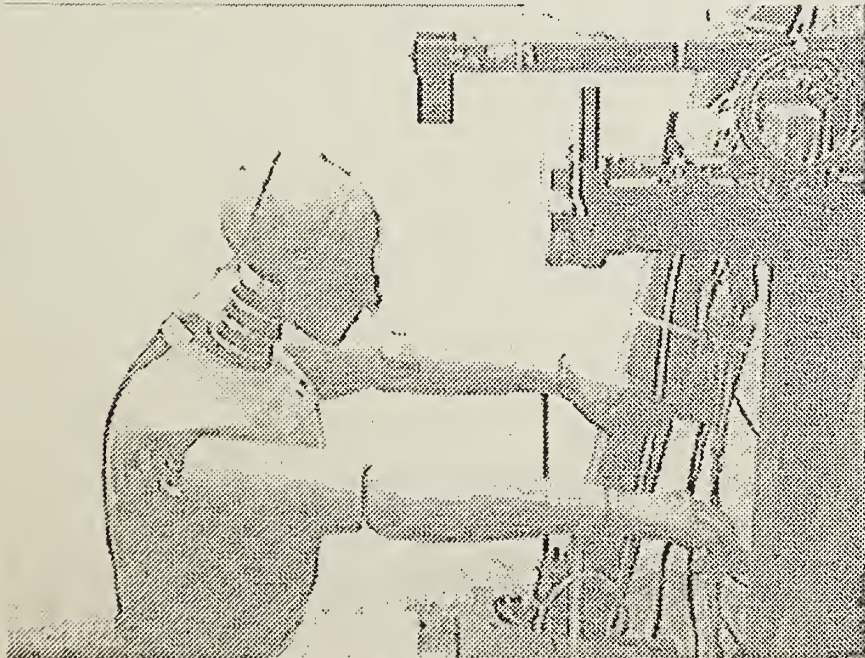


Figure 5 – Direct Impact (Frontal)

2.4 Free-Motion Windshield Impacts

Four tests were conducted with a Free-Motion Headform test device⁵. The test setup appears in Figure 6. A linear ram projected the fully instrumented head into an automotive windshield. The high frequencies generated by the breaking glass were to provide a severe impact environment in which to evaluate the sensors. Testing was performed at 6.7 m/s, 8.9 m/s (2 tests), and 11.2 m/s.

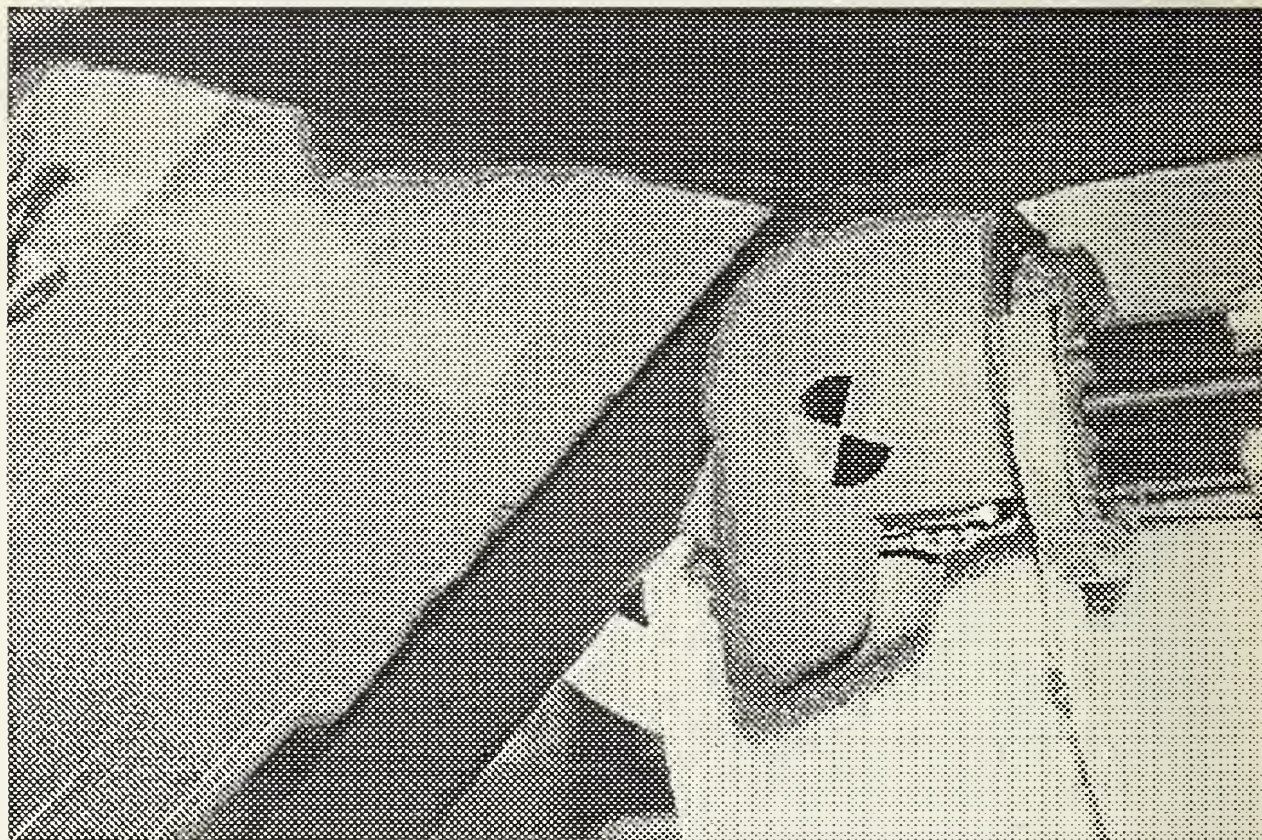


Figure 6 – Free-Motion Headform Projected into Windshield

2.5 Data Handling

All data were collected on SAE Class 1000⁶ channels over the Metraplex Data Acquisition System (MDAS) at the VRTC. The electronics in the AAS-01 sensors incorporate an analog filter which attenuates the signal -3 dB at 500 Hz. This filtering makes the AAS signal analogous to what would be a Class 300 channel (which is not defined). The signals used in the 3-2-2-2 calculations are all Class

1000. A direct comparison between the two angular acceleration measurement methods is therefore distorted by the difference in frequency content between the two signals.

3.0 RESULTS

3.1 Power Supply Noise

The results of the noise tests revealed that the power supplies constructed at the VRTC introduce very little noise into the signal. All three power supply units responded similarly. Without physical input, the signal varies less than $\pm 0.5\%$ of the full scale for both IETL and AAS channels. SAE J211 recommends that the static calibration error be less than 1.5% of the data channel full scale⁶. The frequency content of these signals is dominated by a large spike at 60 Hz, representative of the standard 115 V AC electrical current powering the unit. Figure 7 displays power spectra of three of the AAS sensors and the IETL angular velocity sensor. The IETL spectra shows spikes at much higher frequencies (up to 1500 Hz) than the AAS sensors. This difference is likely a result of attenuation of the AAS-01 channel by its inherent analog filtering. Although the IETL sensor has a frequency response which is -3 dB at 2500 Hz, the Metraplex data acquisition system incorporates SAE Class 1000 filtering: flat to 1000 Hz and -3 dB at 1650 Hz.

3.2 Cross-Axis Sensitivity

The cross-axis sensitivity of both the AAS-01 sensors and the 3-2-2-2 linear accelerometer array was determined using data from the frontal head/neck pendulum testing. Only the frontal tests allowed the cg alignment necessary to ensure nearly planar motion. Both measurement systems were analyzed independently, with the respective Y-axis angular acceleration serving as the reference channel for each. The X- and Z-axis angular accelerations at the time of the peak Y axis angular acceleration were used to determine the percentage error as follows:

$$\left[\frac{\alpha_i @ \text{Max } \alpha_y}{\text{Max } \alpha_y} \right] \times 100$$

$i = x, z$

$\alpha = \text{angular acceleration}$

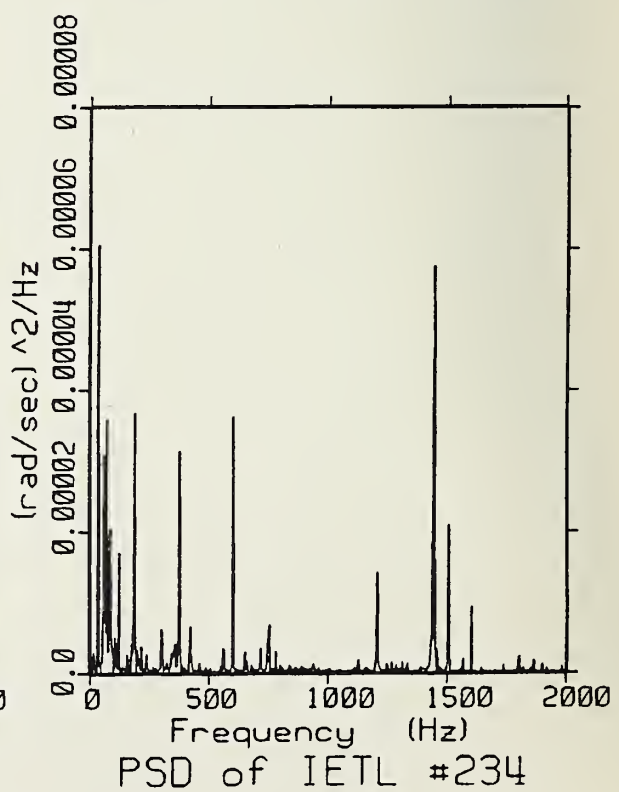
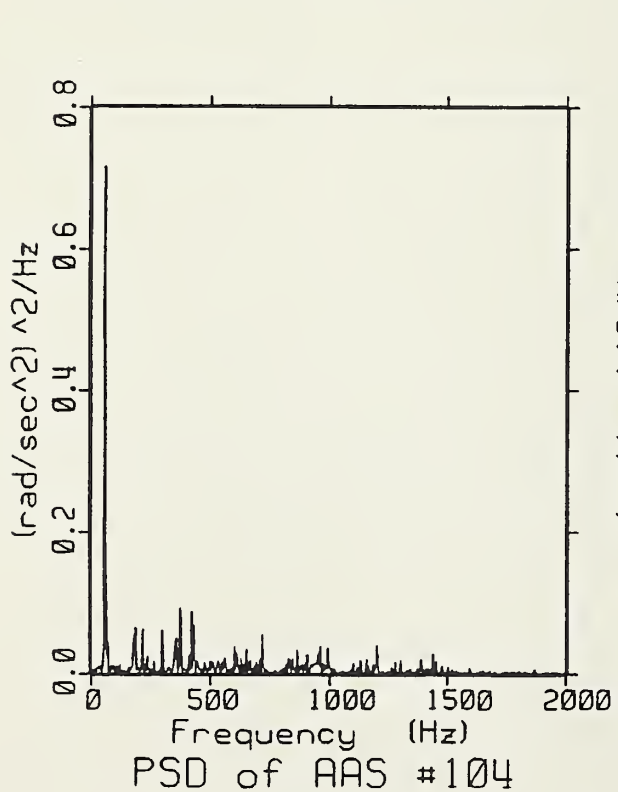
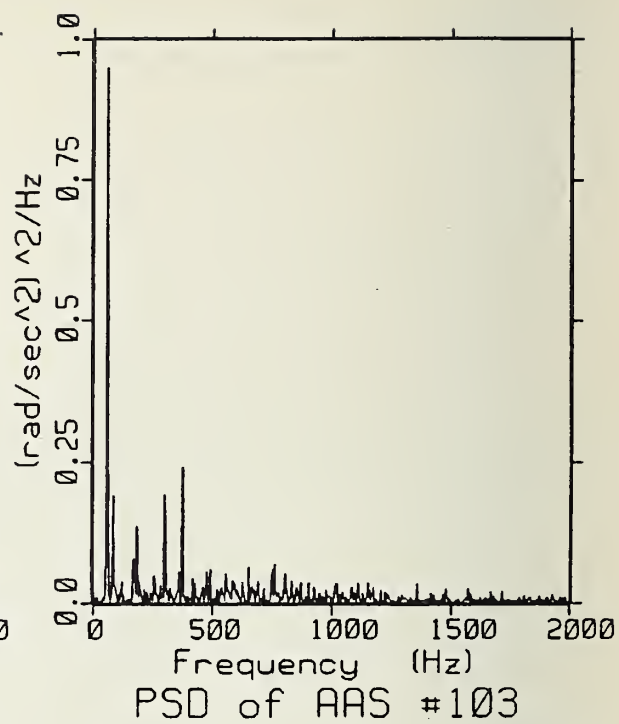
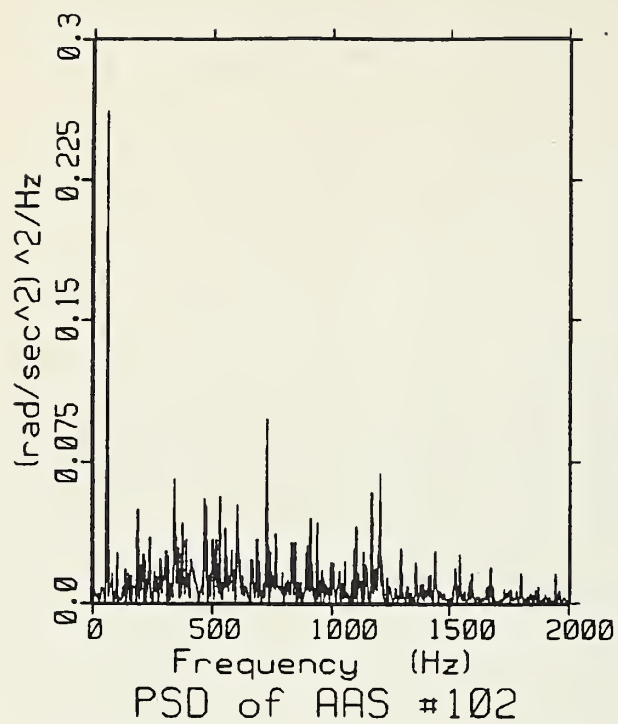


Figure 7 – Power Spectra for Power Supply Noise Tests

Table 1 displays the cross-axis angular errors as calculated for both the AAS-01 and the 3-2-2-2 array.

TABLE 1 – Cross Axis Angular Error

Test #	Cross-Axis	AAS-01 Error	3-2-2-2 Error
02260046	X-Axis	3.4 %	2.4 %
	Z-Axis	3.4 %	0.42 %
02260047	X-Axis	2.5 %	1.2 %
	Z-Axis	2.5 %	1.8 %
02260048	X-Axis	3.4 %	1.8 %
	Z-Axis	0.81 %	1.8 %
Averages:		3.1 %	1.87 %

Appendix A provides the performance specifications for the AAS-01. The 3.1 % average cross axis angular acceleration error found in our testing is slightly higher than that specified by the manufacturer (<2%). The 3-2-2-2 array displayed average cross-axis angular accelerations of nearly 2%. It is possible that some of the cross-axis signal may represent actual angular motion occurring in the pendulum test. The manufacturer's procedure was much more controlled to isolate the rotation to a single axis. It was decided that even if the error values shown in the frontal pendulum test represented true cross-axis angular sensitivity, the values were low enough for further testing to proceed.

3.3 Head/Neck Pendulum Testing

The results of the testing on the Head/Neck Pendulum are shown in Table 2. Y-axis rotations are compared for the frontal tests (02260046-02260048), X-axis rotations for the lateral impacts, and the resultant angular accelerations compared for the oblique impacts (02260052-02260054). The percentage difference calculations are determined from the peak AAS-01 measurement with respect to the nine accelerometer array.

**TABLE 2 – Head/Neck Pendulum Testing
Angular Accelerations AAS-01 vs. 3-2-2-2**

Test #	Orientation	3-2-2-2 rad/sec ²	AAS rad sec ²	% Difference
02260046	Frontal	2455	2468	0.53
02260047	Frontal	2475	2565	3.64
02260048	Frontal	2471	2549	3.16
02260049	Lateral	2185	2175	-0.46
02260050	Lateral	2309	2317	0.35
02260051	Lateral	2327	2309	1.38
02260052	Oblique	2529	2898	14.59
02260053	Oblique	2554	2853	11.71
02260054	Oblique	2401	2697	12.33

The AAS-01 and the 3-2-2-2 angular acceleration signals showed very good correlation. The single channel comparisons for both frontal and lateral tests were all within $\pm 4\%$. The oblique tests which compared resultant angular accelerations were not as close, showing differences of up to 14.6%. The cause for the increased variation between the systems in the oblique tests was not clear. Comparisons along the three individual axes revealed greater measurement differences (for a single axis) than in either the frontal or lateral tests. Figure 8 compares angular acceleration traces from the two measurement systems for the frontal, lateral, and oblique head/neck pendulum tests. All waveforms matched extremely well.

An important consideration in these comparisons is the frequency content of each signal. Analysis of the Class 1000 channels revealed that the energy spectra of both the AAS-01 signal and the 3-2-2-2 calculation are similarly concentrated at very low frequencies (below 60 Hz). As previously mentioned, the AAS-01 sensor has a cut off frequency of 500 Hz. The energy of the signals generated in this test environment appears to be far enough below 500 Hz, such that a direct comparison of the Class 1000 3-2-2 calculation and the "Class 300" AAS-01 sensor is reasonable. Figure 9 shows power spectral densities of the AAS-01 and 3-2-2-2 array angular acceleration signals.

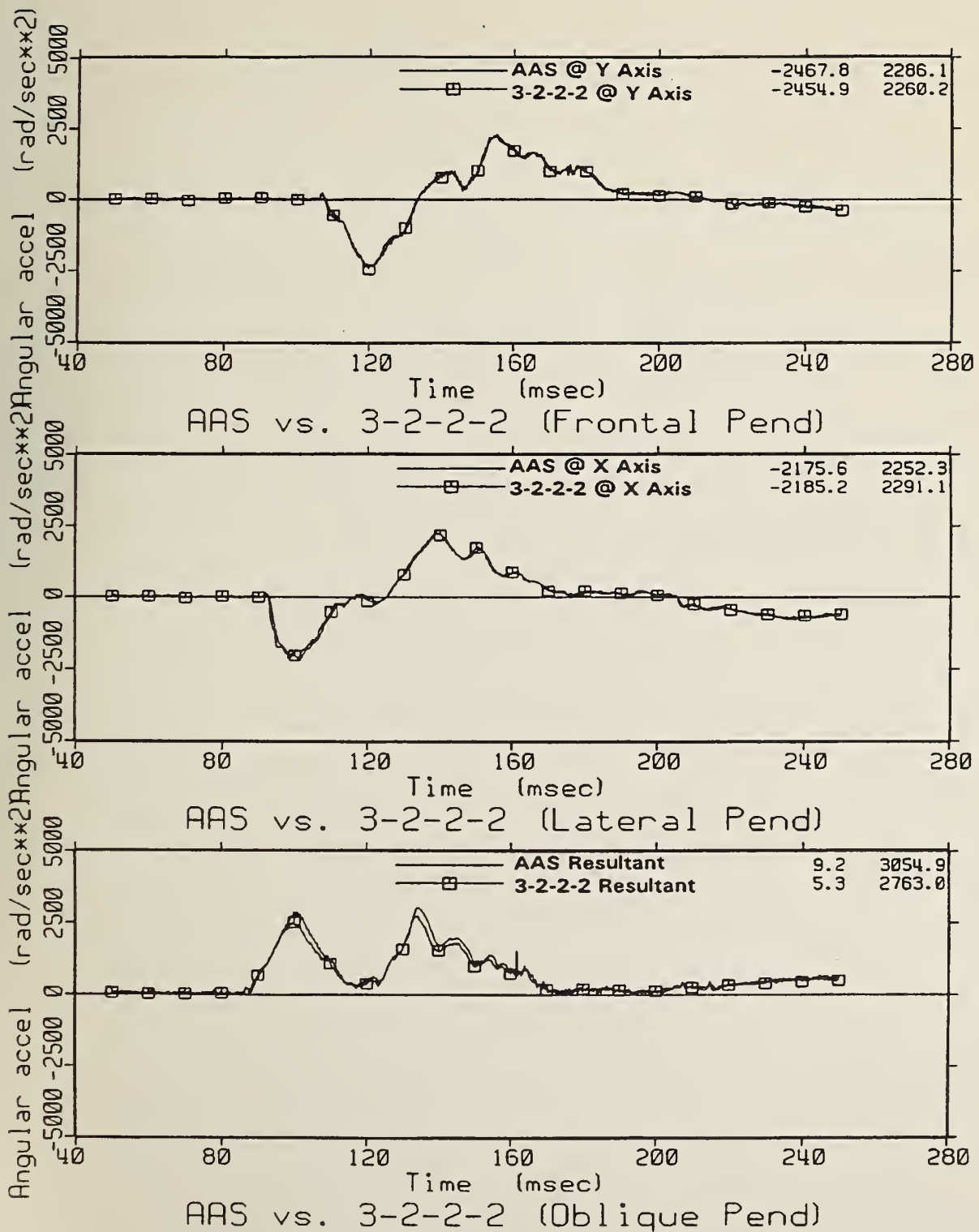
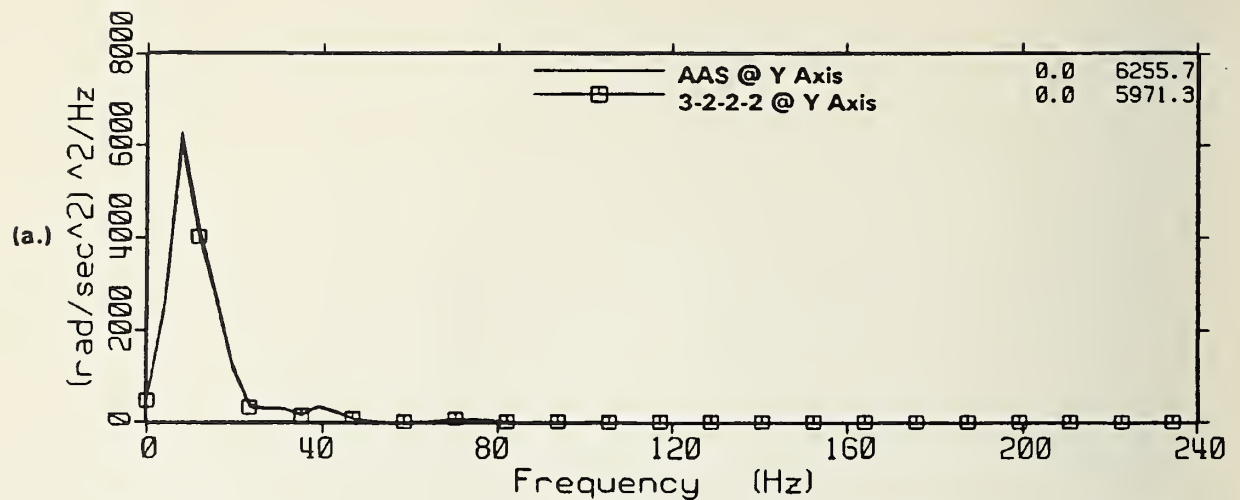
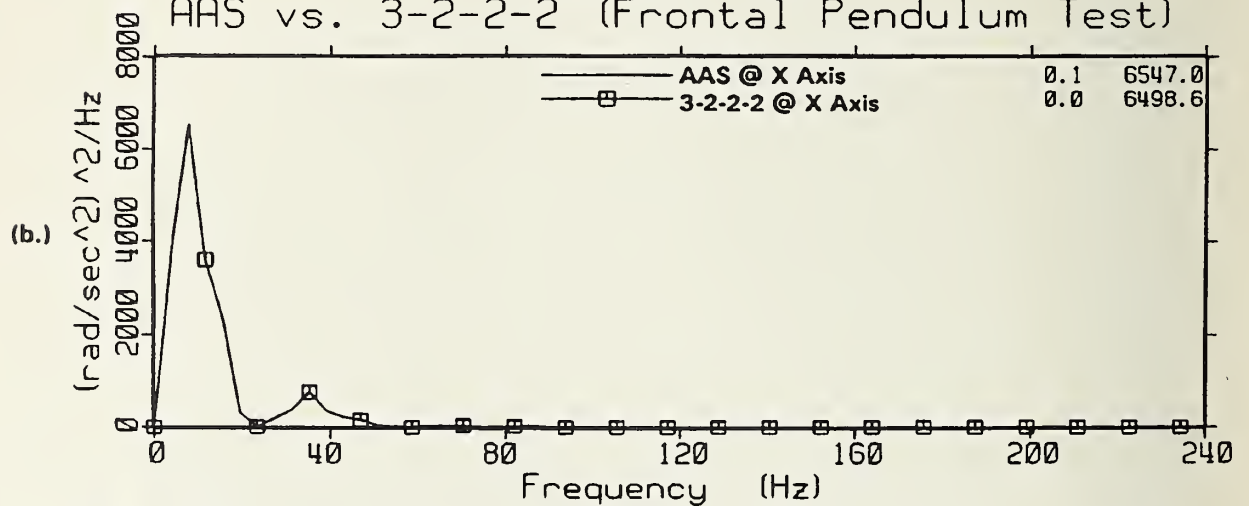


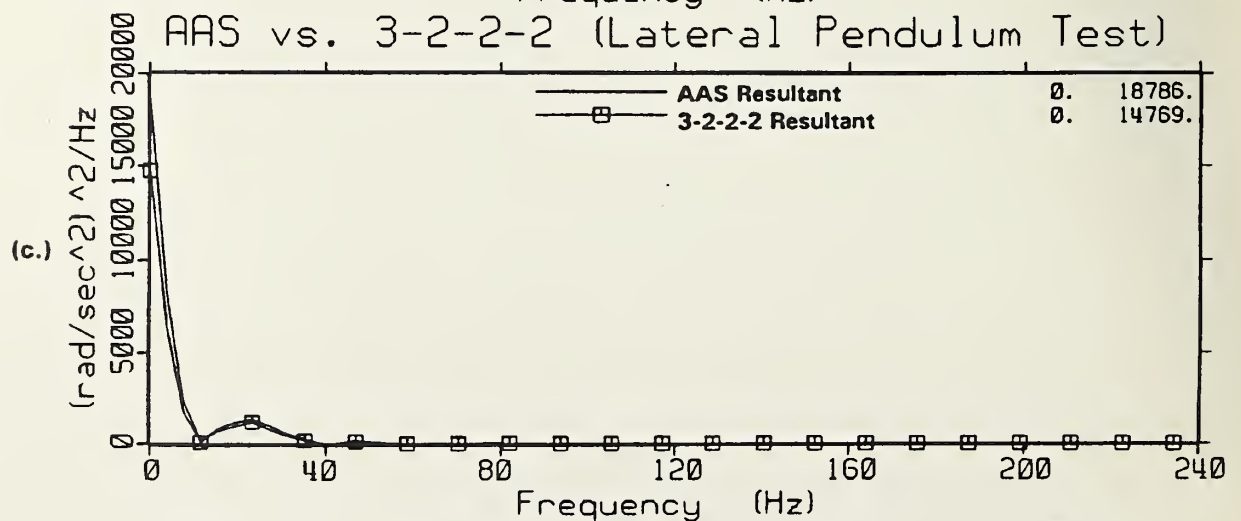
Figure 8 – Head/Neck Pendulum Angular Accelerations



AAS vs. 3-2-2-2 (Frontal Pendulum Test)



AAS vs. 3-2-2-2 (Lateral Pendulum Test)



AAS vs. 3-2-2-2 (Oblique Pendulum Test)

Figure 9 -- Power Spectra from Pendulum Tests

3.3.1 IETL-001 Comparisons to AAS-01 (Analog vs. Digital Differentiation)

Digital differentiation of the IETL-001 angular velocity sensor provided another means of angular acceleration determination, allowing a comparison between analog and mathematical differentiation. Only the three frontal tests were used in this analysis, because only one IETL, measuring y-axis angular velocity (Figure 10a), was included in the head instrumentation package. Differentiation of the unfiltered angular velocity channel produced the angular acceleration curve shown in Figure 10b. The apparent noise introduced by the mathematical differentiation process complicated a direct comparison to the AAS-01 sensor. Because the earlier frequency analysis (see Figure 9) revealed only very low frequencies in the angular acceleration signals, the differentiated IETL channel was filtered to SAE Class 180 ($F_{co}=300$ Hz), with the results shown in Figure 10c. To allow a more direct comparison between analog and mathematical differentiation, the AAS-01 signal was also digitally filtered to Class 180. Table 3 quantifies these comparisons, along with the three y-axis angular accelerations (AAS-01, 3-2-2-2, and differentiated IETL-001) overlaid in Figure 11. In this low frequency test environment, all three Class 180 angular acceleration channels are quite comparable.

TABLE 3 – IETL-001 vs. AAS-01

Test #	AAS-01 Class 1000	AAS-01 Class 180	Differentiated IETL-001 Class 180	% Difference AAS-vs-IETL
02260046	2470	2470	2336	-1.72
02260047	2565	2539	2400	-5.47
02260048	2548	2539	2418	-4.77

3.4 Linear Transfer Pendulum Testing

Table 4 contains the results of direct impacts to the head of a fully assembled dummy. Class 1000 angular accelerations are again compared based on impact direction (see section 3.3).

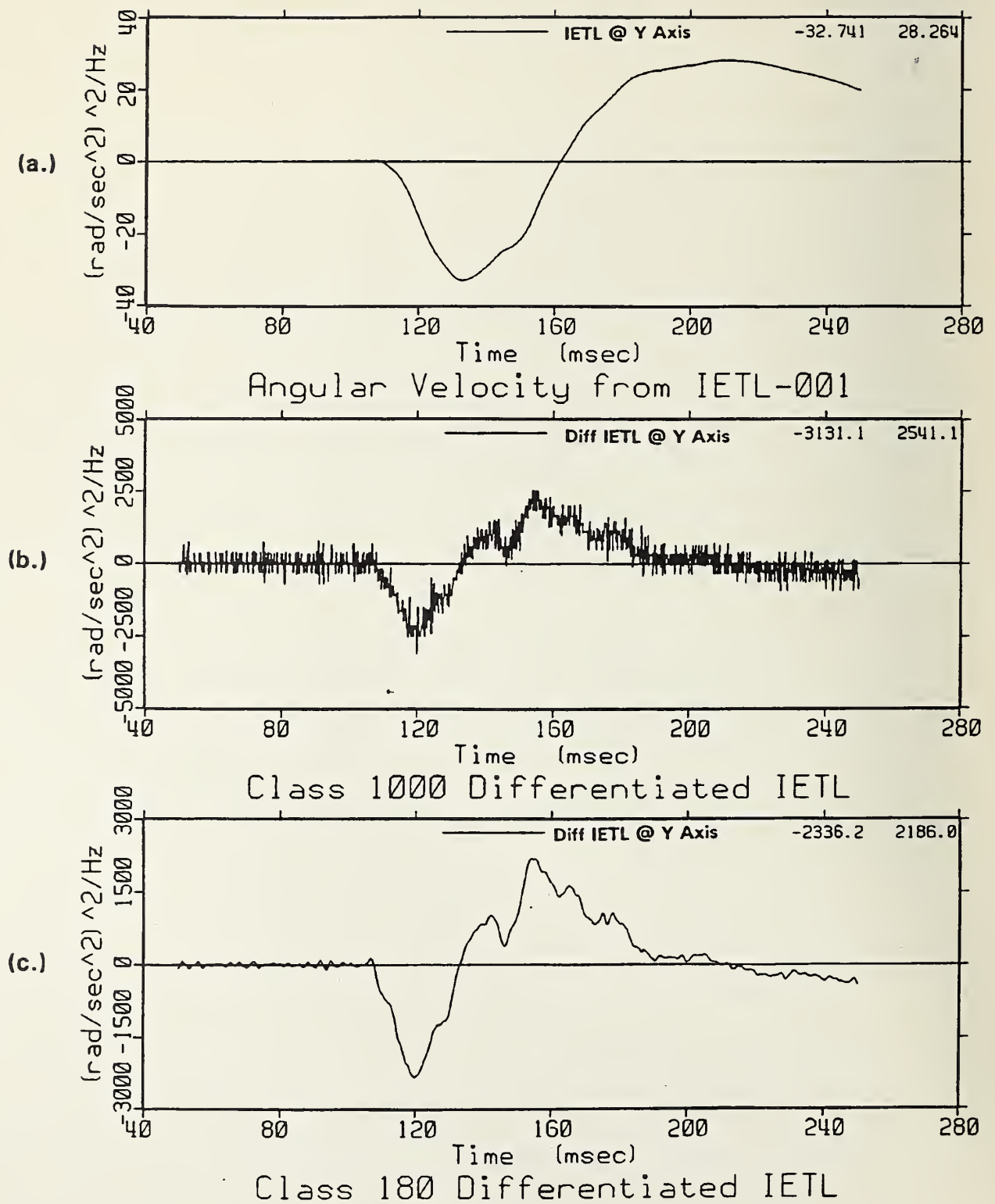


Figure 10 – IETL-001 Angular Velocity Measurement and Differentiation

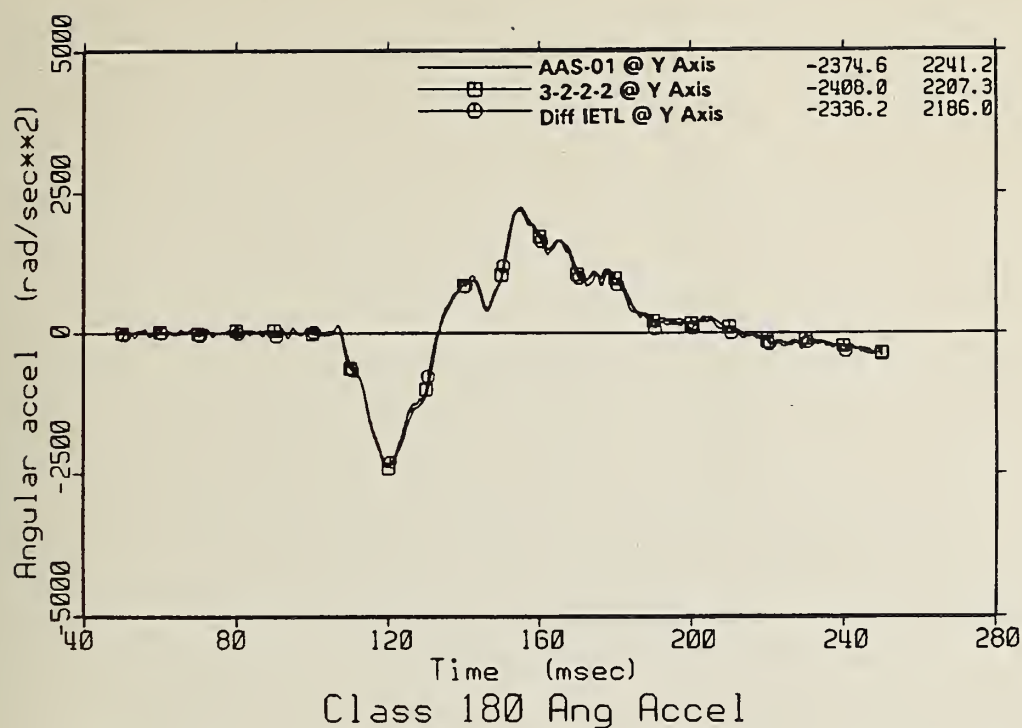


Figure 11 – AAS-01, 3-2-2-2, and Differentiated IETL-001 Ang Accels

TABLE 4 – Direct Head Impacts

Test #	Speed &	3-2-2-2	AAS-01	% Difference
02260055	2.1 m/s Frontal	5967	6175	3.49
02260061	4.3 m/s Frontal	17115	19691	15.05
02260058*	2.1 m/s Lateral	6799*	9280	36.49*
02260059	4.3 m/s Lateral	35741	28704	-19.69
02260057	2.1 m/s 35° Off	7004	9010	28.64
02260060	4.3 m/s 35° Off	19544	28551	46.09

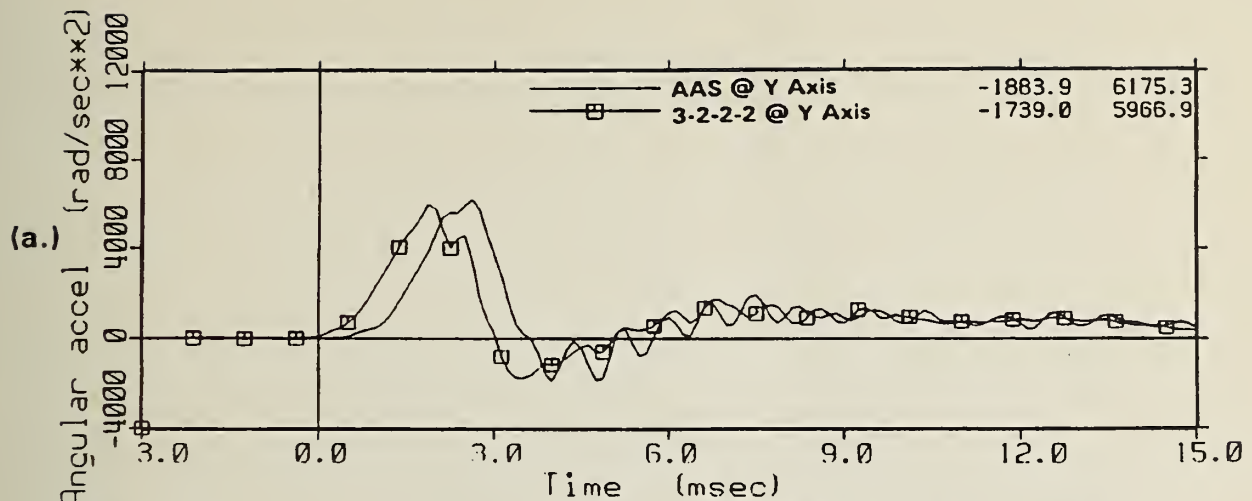
One accelerometer in the 3-2-2-2 array was driven overrange (clipped). To allow a more accurate calculation, the clipped portion of the channel was reconstructed using a sine wave input. The clipped channel, reconstruction, and calculated 3-2-2-2 angular acceleration are provided in Appendix B.

The angular accelerations for the direct impacts showed greater variances than the pendulum tests. Along with the magnitude discrepancies, the AAS-01 signal lagged behind that of the 3-2-2-2 array on every test in this series. The analog filter of the AAS-01 is the likely source of this time shift. Also, in five of the six tests in this series, the AAS-01 sensors recorded higher acceleration values than the 3-2-2-2. Considering the difference in sensor bandwidth, the 3-2-2-2 array could be expected to produce the higher value, if analog filtering of the AAS-01 were the problem. Another source must exist for the magnitude differences. The lack of a true reference angular acceleration prohibits judging which measurement system is more accurate in this environment. Figures 12 and 13 compare the 3-2-2-2 and AAS-01 angular acceleration measurements for the direct head impacts.

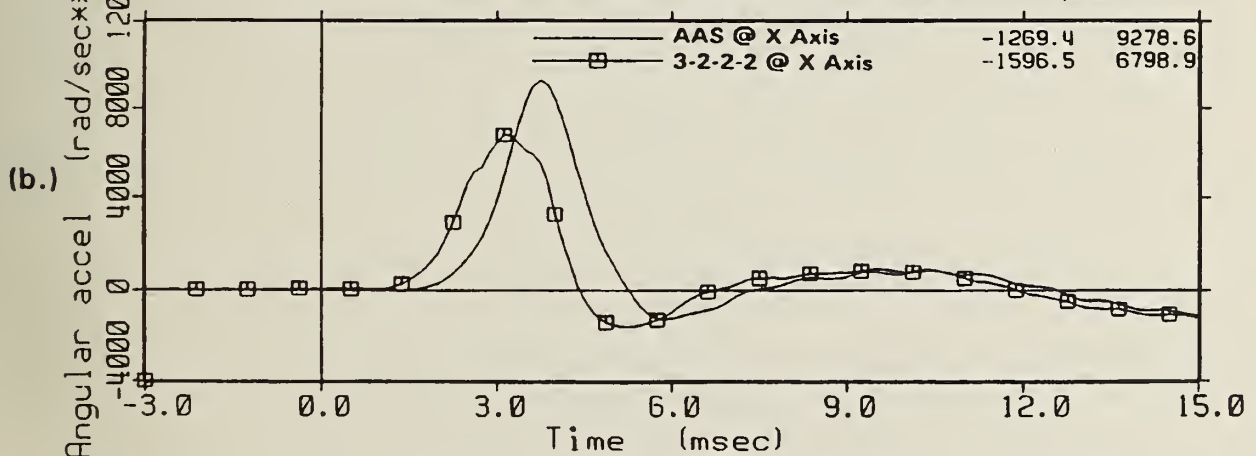
Frequency analysis of these impact tests reveals that much higher frequencies were recorded than in the inertial environment of the head/neck pendulum. As shown in Figure 14, energy of the low speed impacts (2.1 m/s) was present up to approximately 450 Hz. In the high speed impacts, the power spectra extended out to 600 Hz (Figure 15). The power spectrum for test 02260059 (Figure 15b) reveals frequencies, although at low magnitudes, in the range of 900 Hz. Only in this test did the nine-accelerometer array record a higher angular acceleration than the AAS-01. The analog filtering (-3dB @ 500 Hz) of this MHD sensor presumably attenuated the higher frequencies excited in this impact, resulting in a decreased magnitude for the AAS-01 angular acceleration measurement.

3.5 Free-Motion Windshield Impacts

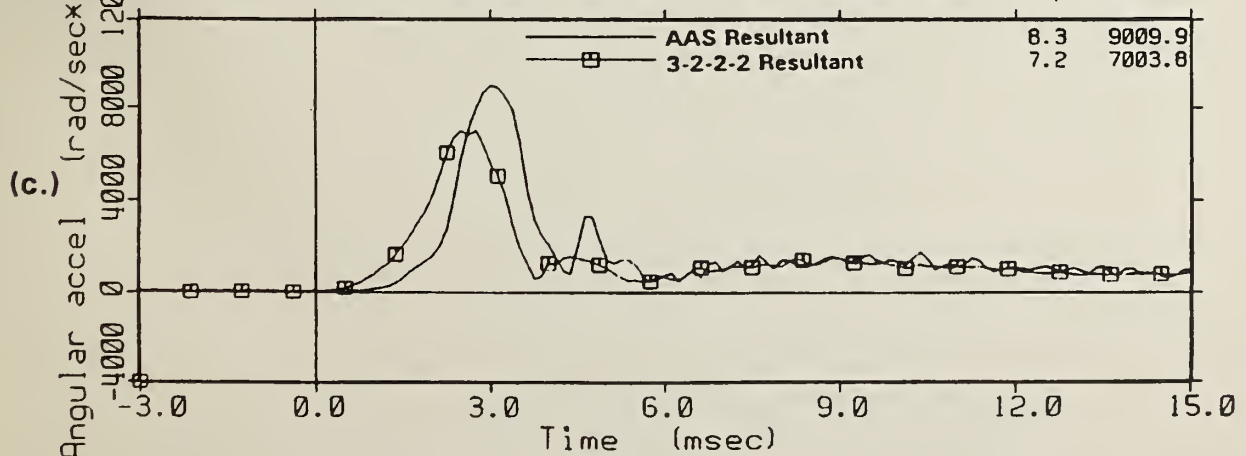
The results of the windshield impacts were difficult to interpret. All comparisons using data from this test series are qualitative and consider only the y-axis angular accelerations. While the impact of the free motion headform into the windshield is not strictly planar, rotation occurs predominantly within the X-Z plane (see fig 1). The Z-axis AAS-01 angular acceleration measurement showed very high frequency oscillations. Mounting of the Z-axis AAS-01 was not as stable as along the other axes (see Figure 2) and likely contributed to the distorted signal shown in Figure 16. This signal shows the dampening characteristics of vibration. Because of the potential effect of this channel on the AAS-01 resultant calculation, it was determined that y-axis accelerations alone would provide a better comparison.



AAS vs. 3-2-2-2 (2.1 m/s Frontal Impact)



AAS vs. 3-2-2-2 (2.1 m/s Lateral Impact)



AAS vs. 3-2-2-2 (2.1 m/s Oblique Impact)

Figure 12 – Low Speed Direct Impact Angular Accelerations

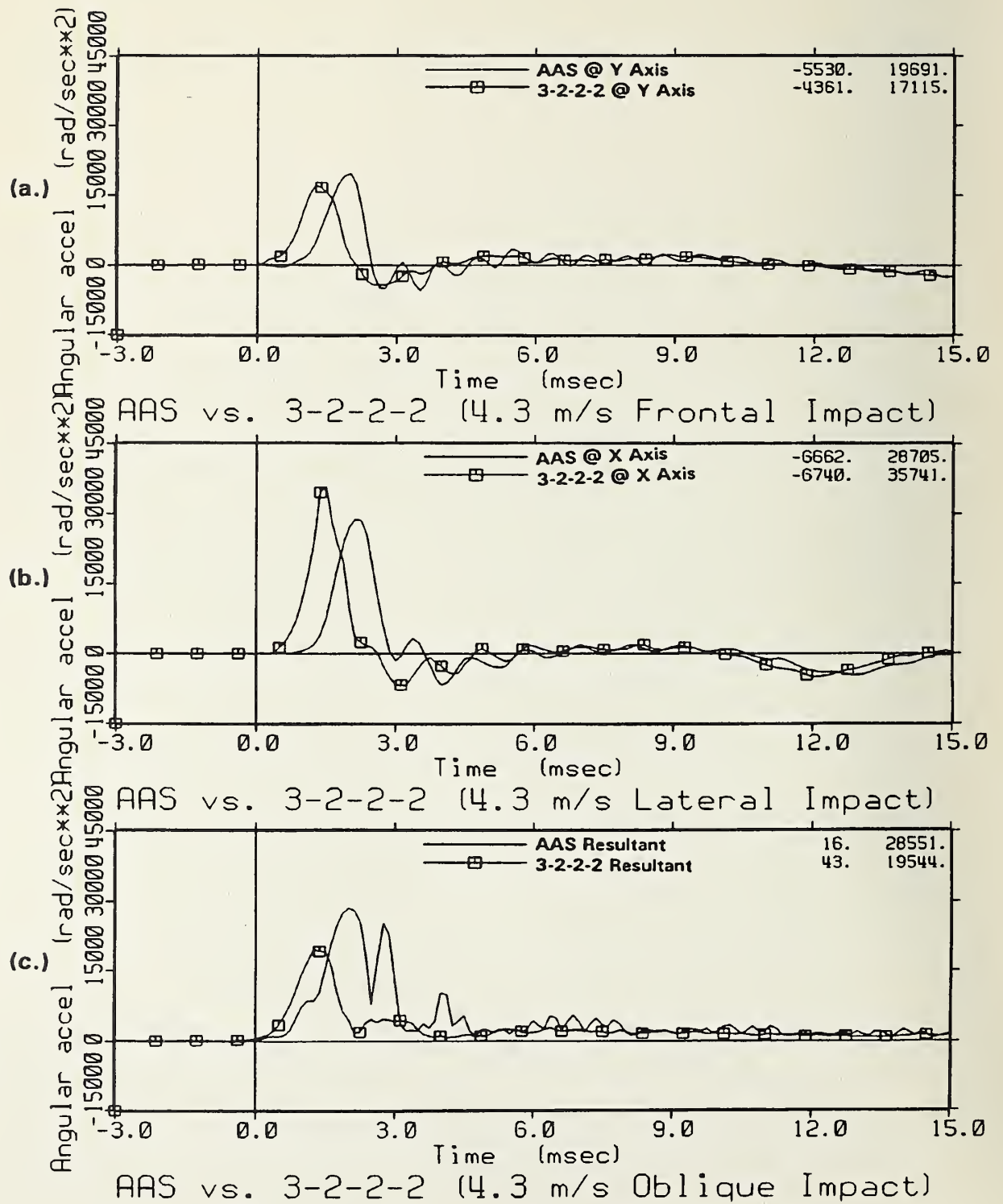
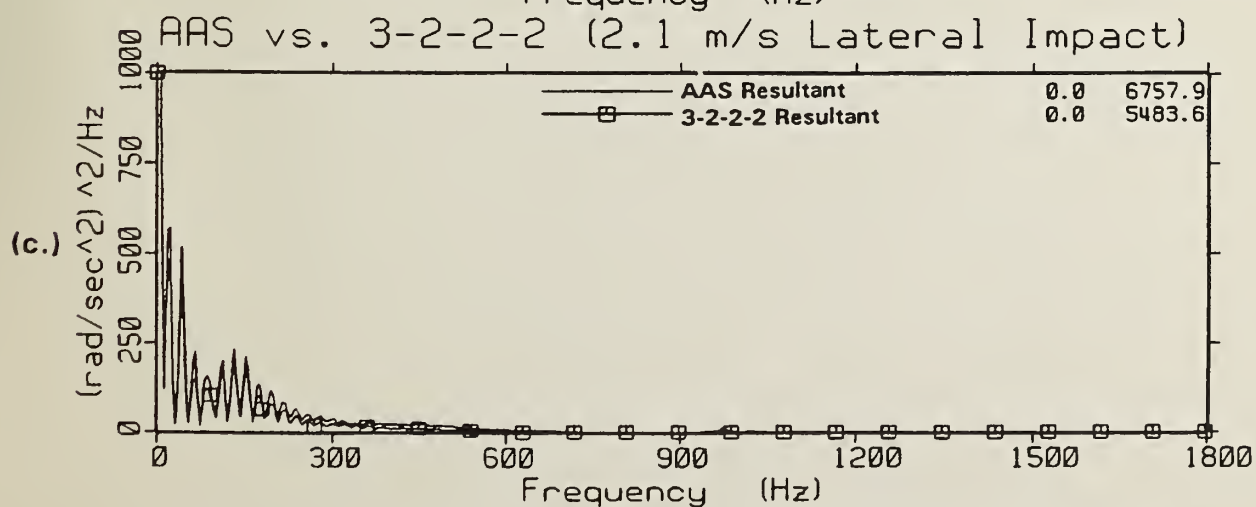
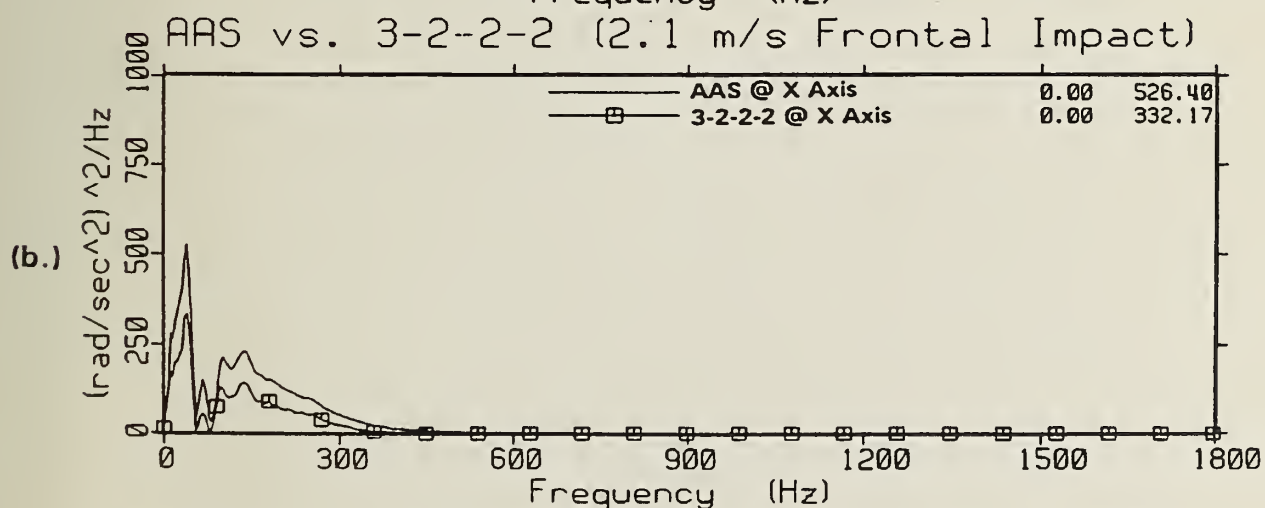
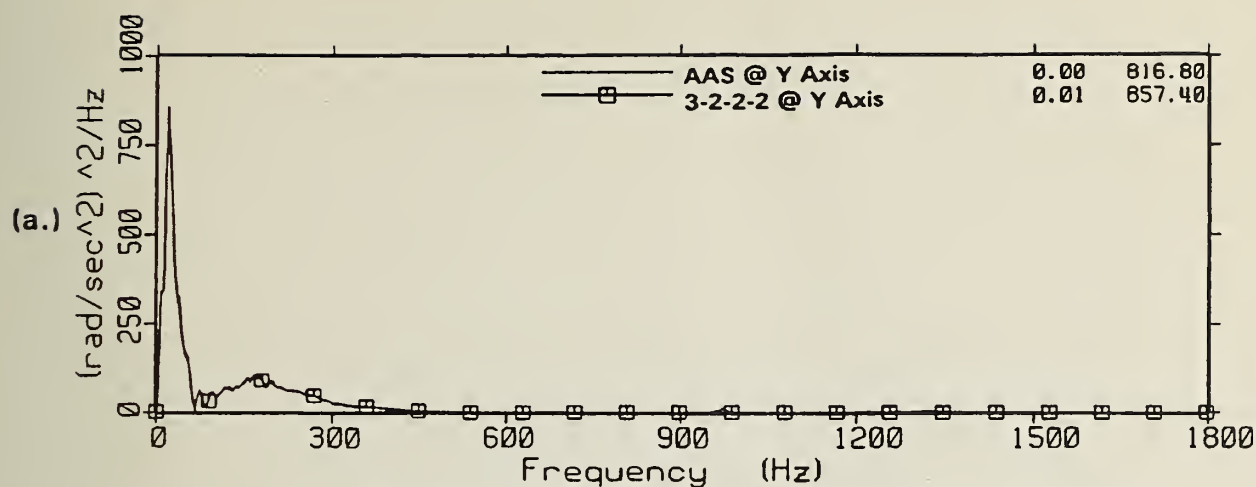
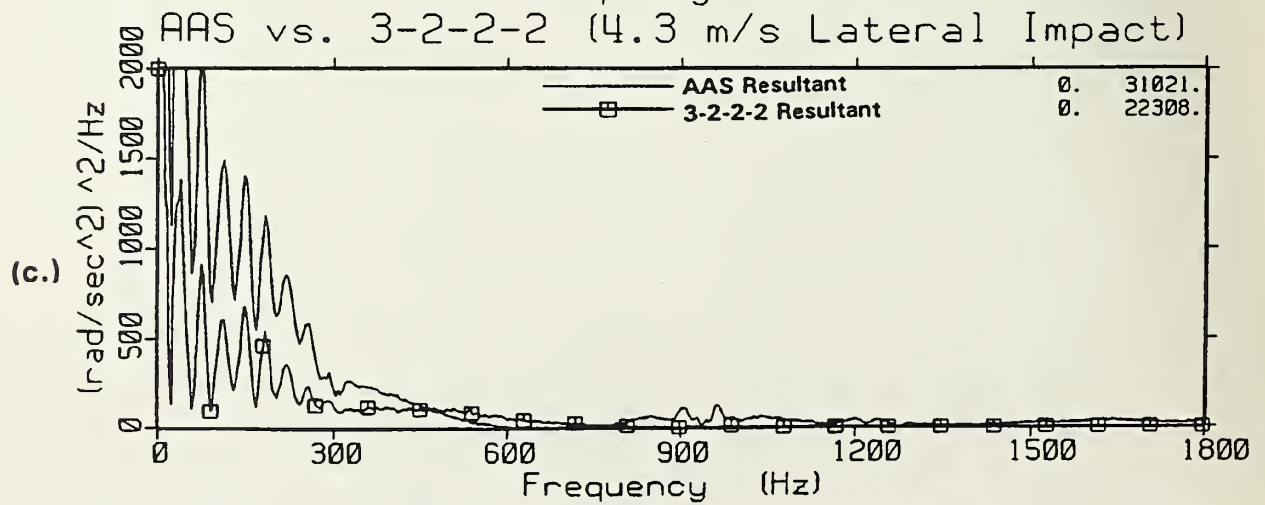
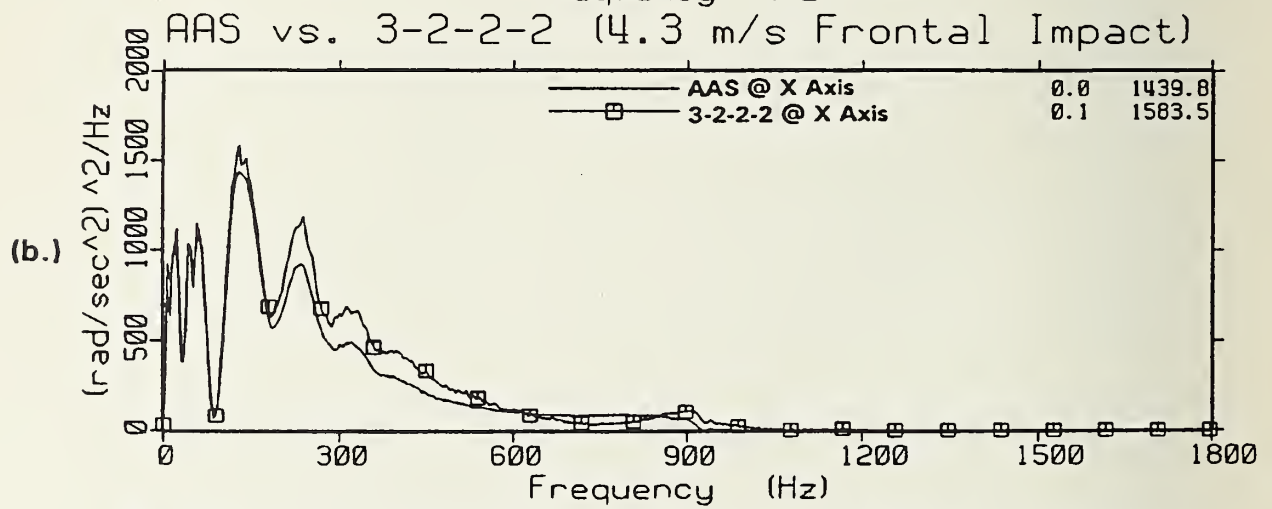
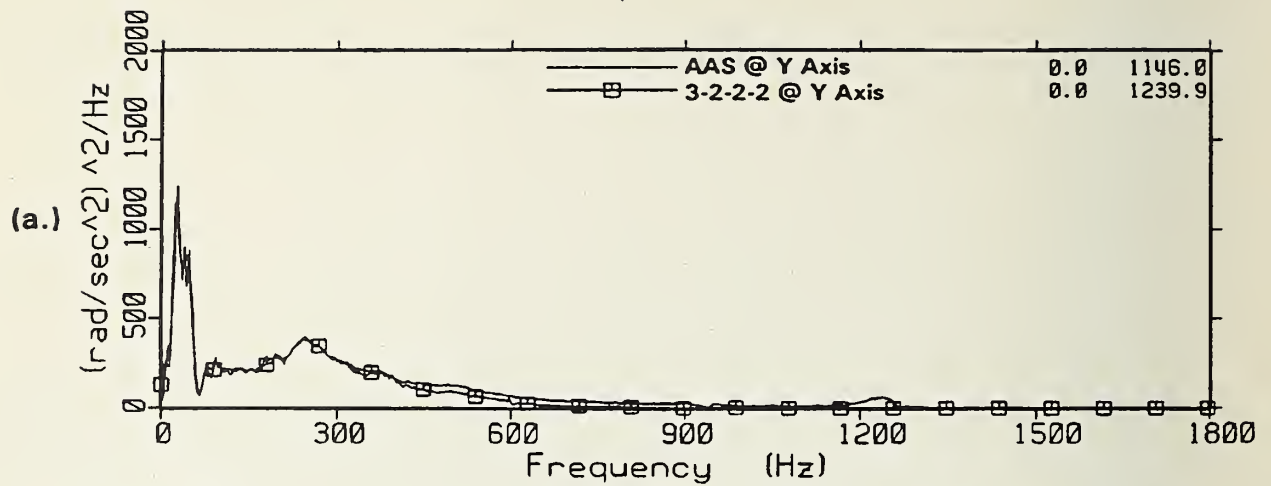


Figure 13 – High Speed Direct Impact Angular Accelerations



AAS vs. 3-2-2-2 (2.1 m/s Oblique Impact)

Figure 14 – Power Spectra for Low Speed Linear Impacts



AAS vs. 3-2-2-2 (4.3 m/s Oblique Impact)

Figure 15 – Power Spectra for High Speed Linear Impacts

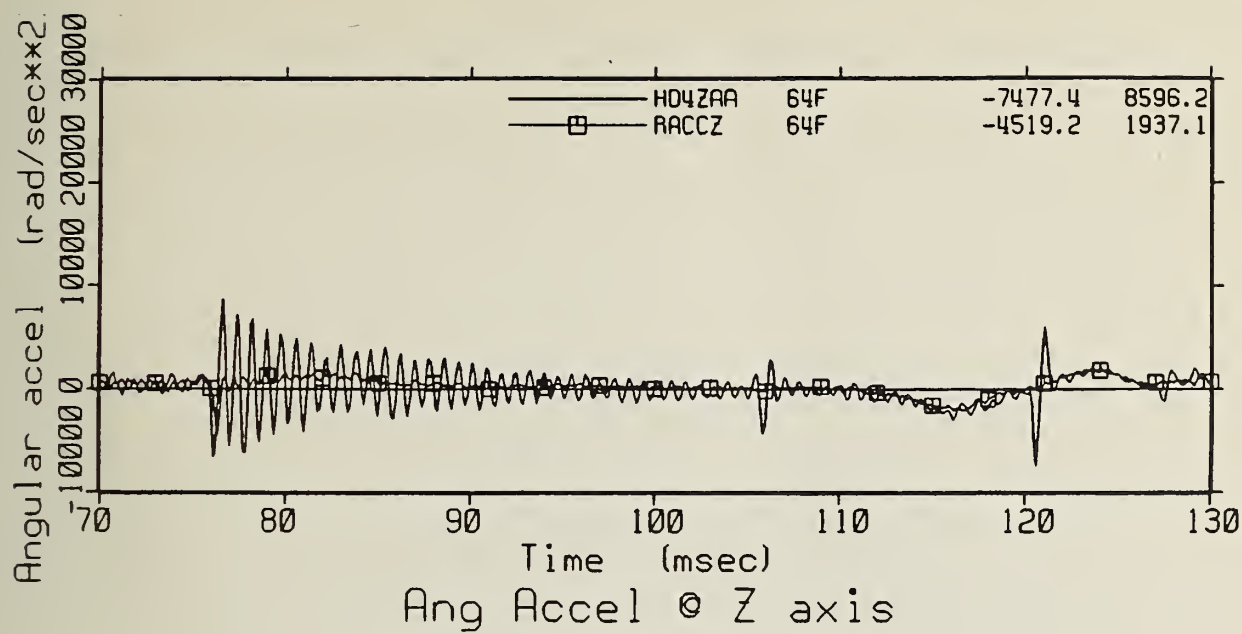


Figure 16 -- Ringing of Z-Axis AAS-01

Figure 17 compares the angular acceleration from the AAS-01 and the nine-accelerometer array. Traces of the AAS-01 signals display high frequency oscillations, consistent for all four tests. Frequency analysis revealed energy in the AAS-01 signal between 1000 Hz and 1500 Hz. This is somewhat evident in the power spectra shown Figure 18, particularly 18a and 18d. As previously mentioned, analog filtering of the AAS-01 attenuates the signal -3 db at 500 Hz. For energy to be evident in the AAS-01 at the high frequencies shown, the undamped magnitude must have been quite high. Figure 19 shows a narrow window of the power spectra, revealing that the 3-2-2-2 array, with a 1650 -3db point, did not sense similar energy. The high frequency energy of the AAS-01 signal was likely a result of mechanical vibration of the sensor mount, or perhaps resonance in the sensor itself.

Despite the AAS-01 oscillatory characteristic, the shape of the two angular acceleration traces were comparable. A phase shift similar to that seen in the direct impacts, with the 3-2-2-2 leading, is also evident. Figure 17b displays a large spike in the 3-2-2-2 angular acceleration. Analysis of individual linear accelerometer channels revealed several spikes which may have been compounded in the 3-2-2-2 angular acceleration algorithm. Dismissing the high frequency AAS-01 content previously described as vibration, the energy of both signals is concentrated below 200 Hz.

4.0 DISCUSSION

The above sections report the results of testing, comparing angular accelerations as determined by both the 3-2-2-2 and AAS-01 measurement systems. A major obstacle in the analysis of these comparisons is the lack of a true reference angular acceleration by which to gage the performance of the respective systems. Previous studies^{7,8} have cited four major areas of concern with the nine accelerometer array: transverse (cross axis) sensitivity, mismatch of accelerometer pairs, misalignment of accelerometers, and signal noise. The AAS-01 sensor has never before been tested in the impact environment. This study provides information on how the two systems perform with respect to each other, without being able to determine which is more accurate. The comparisons are further complicated by the inherent analog filtering of the AAS-01 sensors.

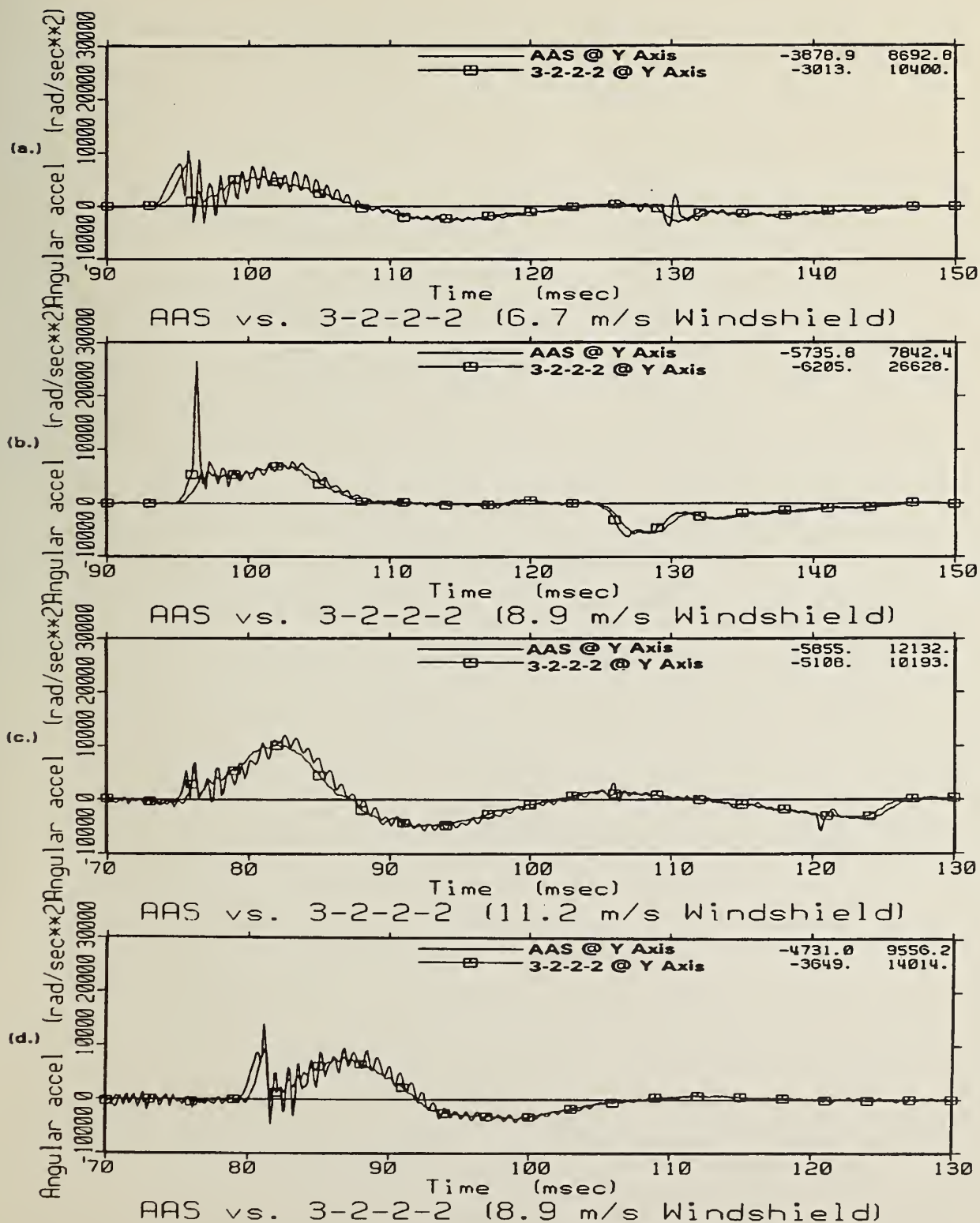


Figure 17 – Angular Accelerations from Windshield Impacts

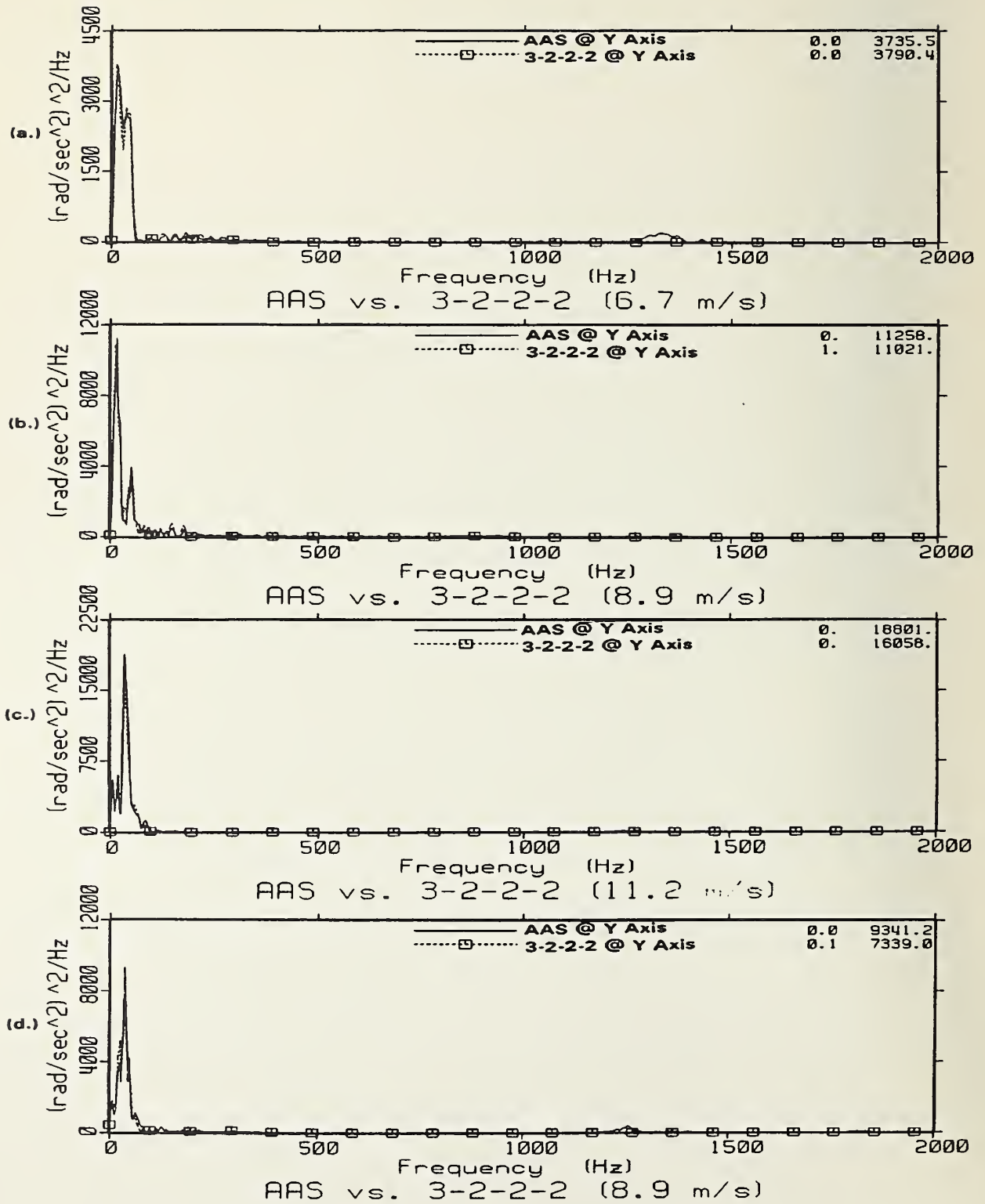


Figure 18 – Power Spectra for Windshield Impacts

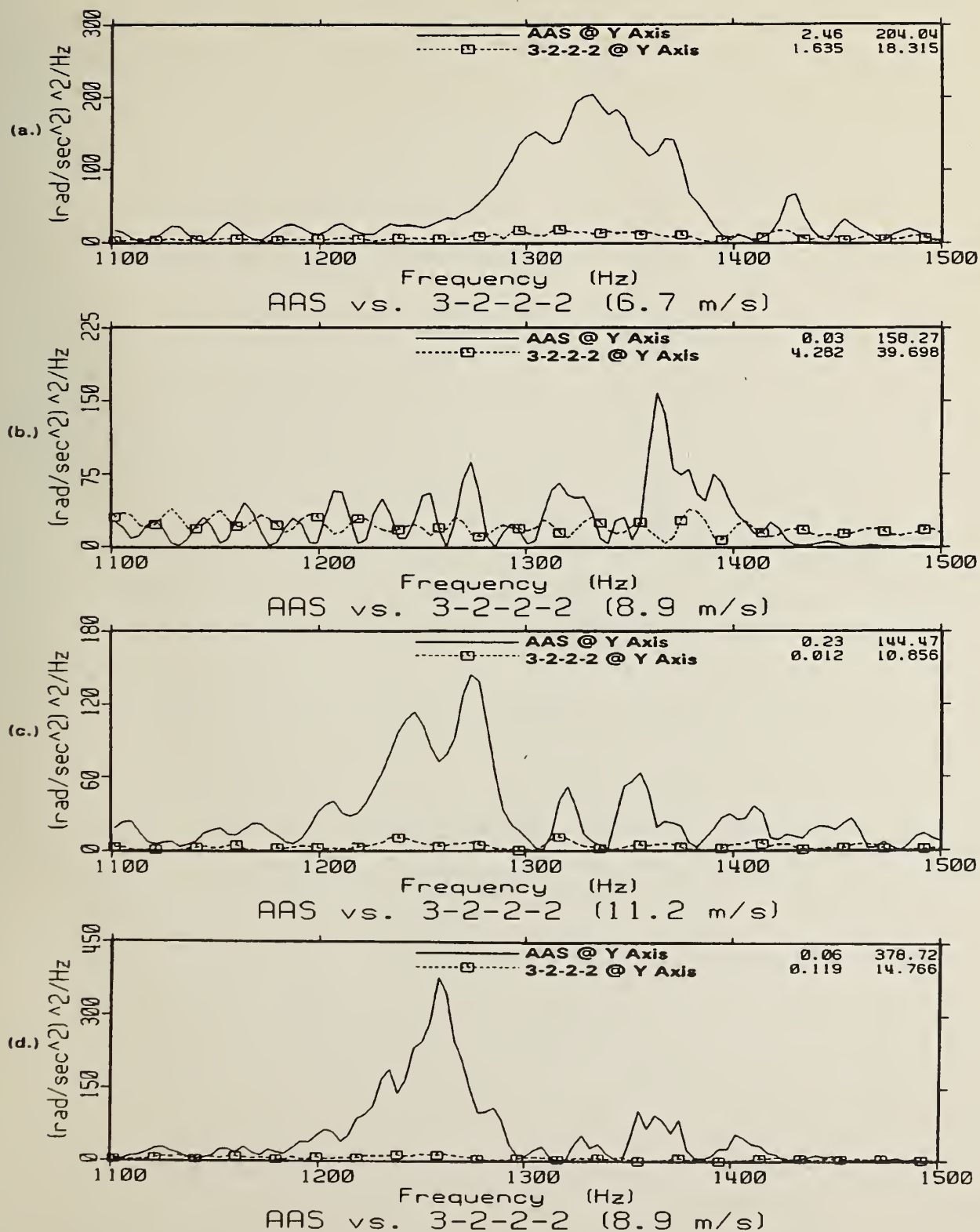


Figure 19 – Narrow View of High Frequencies from Windshield Impacts

Throughout this program, the frequencies experienced by the head in each environment were carefully considered. In the study using IETL-001 sensors at NBDL², it was suggested that SAE Class 180 channels may be sufficient to capture all significant energy for head rotational motion for their sled tests. The Class 180 Butterworth filter on the VAX System at the VRTC has the stop band at 750 Hz. The energy levels experienced by the head in the direct impact tests extended into much higher frequencies than the NBDL tests. The frequency spectra were more closely examined to determine which filter class might be appropriate for impact tests measuring head angular acceleration.

The angular acceleration signals from both the AAS-01 sensors and the 3-2-2-2 array were filtered to SAE Class 600 and SAE Class 180 to explore the effects of filtering on the data from different test environments. The pendulum and direct impacts were both considered. The windshield impacts were excluded from this analysis because of the presence of mechanical resonance as noted in section 3.5. The 3-2-2-2 array and AAS-01 signals were evaluated independently by determining the difference in peak angular acceleration of the Class 600 and Class 180 channels from the peak angular acceleration collected at Class 1000. Tables 5 and 6 outline these results for the AAS-01 sensors and the 3-2-2-2 array, respectively.

These tables suggest that SAE Class 180 head angular acceleration channels may be sufficient for head/neck pendulum testing. However, for the direct head impacts, as much as 30% of the real signal magnitude may be attenuated at this filtering level. The Class 600 channel appears to offer a much better signal, with the average difference (with respect to Class 1000) of 3% noted for the 3-2-2-2 data from the direct impacts. The AAS-01 data from both pendulum and direct impacts, as well as the 3-2-2-2 pendulum data, all averaged less than 1% loss in peak magnitude from the Class 1000 channel. Direct contact to the dummy head occurs in a variety of test exposures and must be accounted for when considering appropriate instrumentation and data processing. Dummy head angular accelerations should be analyzed as at least SAE Class 600 channels, as lower filtering corridors may significantly attenuate these signals.

TABLE 5 – Filtering of AAS-01 Angular Acceleration

Test #	Class 1000	Class 600	% Diff	Class 180	% Diff
Head/Neck Pendulum Tests					
02260046	2468	2440	-1.13	2376	-3.73
02260047	2565	2552	-0.51	2474	-3.55
02260048	2892	2547	-0.08	2539	-0.39
02260049	2175	2166	-0.41	2139	-1.66
02260050	2317	2313	-0.17	2281	-1.55
02260051	2359	2353	-0.25	2336	-0.97
02260052	2898	2359	-1.45	2829	-2.38
02260053	2853	2835	-0.63	2818	-1.23
02260054	2697	2672	-0.93	2552	-1.45
Average Difference @ Class 600 = -0.68%				@ Class 180 = -1.88%	
Direct Head Impact Tests					
02260055	6175	5991	-2.98	4873	-21.09
02260061	19691	19244	-2.27	11169	-43.28
02260058	9280	9214	-0.71	7373	-20.55
02260059	28704	28753	0.17	18384	-35.95
02260050	9280	9025	0.17	6995	-22.36
02260060	28551	29371	2.87	15553	-45.53
Average Difference @ Class 600 = -0.46%				@ Class 180 = -31.46%	

TABLE 6 – Filtering of 3-2-2-2 Angular Acceleration

Test #	Class 1000	Class 600	% Diff	Class 180	% Diff
Head/Neck Pendulum Tests					
02260046	2185	2451	-0.16	2457	-1.96
02260047	2475	2487	0.48	2487	-0.04
02260048	2471	2457	-0.57	2323	-1.94
02260049	2185	2159	-1.19	2071	-4.16
02260050	2310	2304	-0.22	2263	-1.94
02260051	2327	2323	-0.17	2310	-0.73
02260052	2529	2489	-1.58	2450	-1.94
02260053	2554	2543	-0.43	2523	-1.21
02260054	2401	2380	-0.37	2380	-0.87
Average Difference @ Class 600 = -0.52%				@ Class 180 = -1.63%	
Direct Head Impact Tests					
02260055	5967	5614	-5.92	4679	-21.59
02260061	17115	16838	-1.62	10631	-37.88
02260054	6799	6688	-1.63	5895	-13.30
02260059	35741	32808	-8.21	19640	-45.05
02260057	7004	6999	-0.07	5751	-17.89
02260059	19544	19471	-0.37	12912	-33.93
Average Difference @ Class 600 = -2.97%				@ Class 180 = -28.27%	

Future testing of head rotational measurement systems should evaluate the package through a variety of impact exposures, representative of typical ATD test environments. Particular attention should be paid to the frequency spectra experienced by the electronics to obtain an optimal signal either through data acquisition or mathematical post-test data processing. SAE J211b currently recommends Class 1000 channels for both linear and angular accelerations. The data presented in this document suggest that a Class 600 channel would suffice for the angular acceleration measurement, without significant signal attenuation. Also, the "Class 300" analog filtering of the AAS-01 sensor is not appropriate for these applications.

The performance of the MHD sensors was highly dependent upon its mounting within the skull. This fact became particularly evident in the windshield tests as presented in section 3.5. The AAS-01 sensors showed a high frequency vibration not picked up by the nine-accelerometer array, leading to the conclusion of mechanical resonance of the mount as the source of the ringing.

The prototype AAS-01 sensor evaluated in this study provides only angular acceleration output via the on-board differentiator. Many users of the IETL-001 sensor integrate the signal to obtain angular displacement data. The AAS-01 signal would require two integration processes to yield angular displacement. Incorporating the analog electronics into an external signal conditioning unit would provide greater flexibility for the rotational sensor user.

An in-line circuit box was constructed which allowed analog differentiation of the IETL-001 signal without sacrificing direct output of angular velocity. Preliminary testing with this differentiator revealed promising results. The angular acceleration obtained through analog differentiation of the IETL-001 signal corresponded very well to both the digital differentiation of this signal and the angular acceleration recorded by the AAS-01. It appears that a similar approach could be taken by the manufacturer to customize the sensor for various applications. A modular in-line unit would allow great variability in transducer characteristics from the same basic sensing element. Also, by eliminating the need for micro-miniature electronics, the cost of the sensor should decrease.

The linear acceleration sensitivity of the AAS-01 sensor is listed as $< 1 \text{ (rad/sec}^2\text{)}/g$ by ATA (Appendix A). In an attempt to verify the translational sensitivity, three AAS-01 sensors and three linear accelerometers were mounted onto the face of a linear impactor. The impactor was guided by a linear

bearing and manually accelerated into the piston's brakes. The Endevco 7264/2000g accelerometers have a listed off-axis linear acceleration sensitivity of $<2\%$. With the Endevco accelerometers accepted as a linear reference, off-axis linear accelerations between 25 and 30% of the thrust were recorded. It was clear that the apparatus used for these tests did not isolate linear acceleration about one axis. These impacts were therefore not used to evaluate the sensitivity the AAS-01 sensors to linear acceleration. The NBDL sled tests revealed low linear acceleration sensitivity for the MHD angular velocity sensors². As the sensing element was identical to that used in the IETL-001, evaluated by NBDL, the translational sensitivity of the AAS-01 was assumed to also be low.

A final point for discussion relates to the calibration of the AAS-01 sensors. The ATA calibration procedure for the IETL-001 sensors has been previously questioned². Of the fifteen tests (nine pendulum and six direct impacts) for which the peak angular accelerations were compared, all except two recorded higher measurements from the AAS-01 sensors. A calibration error would drive all AAS measurements in a consistent direction and may have accounted for some of the differences. It is doubtful, however, that faulty calibration, of either the 3-2-2-2 system, where each accelerometer is individually calibrated, or the AAS-01 sensors, could completely account for the large magnitude differences seen in the impact tests.

5.0 CONCLUSIONS

Based upon the work described in this report, the following conclusions were reached:

- SAE Class 600 channels are the minimum required to capture all significant data for determination of head angular acceleration in common ATD test environments. Greater levels of filtering may result in attenuation of the signal.
- The AAS-01 sensor provides an angular acceleration signal comparable to that obtained through the 3-2-2-2 nine accelerometer package in low frequency head/neck pendulum testing.

- In the higher frequency direct head impacts, the AAS-01 produced a markedly different signal than the 3-2-2-2 array. The lack of a true reference angular acceleration prevented concluding which system was more accurate.
- The AAS-01 MHD sensors are very sensitive to vibrations in the mounting system. In the windshield experiments, the AAS-01 sensors, weighing 46 grams each, showed oscillations characteristic of mechanical resonance. In future work with MHD sensors, careful attention must be paid to the stability of the transducer's mount. It would also be helpful to better understand the inherent resonance characteristics of the sensor.
- Incorporating analog filtering with an in-line external circuit may be advantageous over placing the electronics within the sensor housing. Potential benefits include greater flexibility in signal conditioning and lower cost.

6.0 REFERENCES

1. Laughlin, D.R., *A Magnetohydrodynamic Angular Motion Sensor for Anthropomorphic Test Device Instrumentation*, Proceedings of the Thirty- Third Stapp Car Crash Conference, Society of Automotive Engineers, Warrendale, Pa., 1989.
2. Willems, G.C., Knouse, D.R., *A Detailed Evaluation of the ATA Angular Motion Sensor in Realistic Simulated Crash Environments*, Proceedings of the Thirty-Fifth Stapp Car Crash Conference, Society of Automotive Engineers, Warrendale, PA, 1991.
3. Seeman, M.R., Muzzy, W.H., Lustick, L.S., *Comparison of Human and Hybrid III Head and Neck Response*, Proceedings of the Thirtieth Stapp Car Crash Conference, Society of Automotive Engineers, Warrendale, PA., 1986.
4. Padgoankar, A.J., Krieger, K.W., King, A.I., *Measurement of Angular Acceleration of a Rigid Body Using Linear Accelerometers*, **Journal of Applied Mechanics**, Vol. 42, No. 3, pp. 552-556, September, 1975.

5. Saul, R.A., Farson, M., Guenther, D.A., *Component Head Test Accident Reconstruction Feasibility Analysis*, DOT HS 807 000, Final Report, January, 1986.
6. SAE J211 OCT88, *Instrumentation for Impact Test*, SAE Recommended Practice, 1991 SAE Handbook, Volume 4: On-Highway Vehicles & Off-Highway Machinery, Society of Automotive Engineers, Inc., Warrendale, PA, 1991.
7. Johnson, A.K., Hu, A.S., *Review of Head Rotational Measurements During Biomechanical Impact Tests*, DOT HS 802568, Final Report, 1977.
8. Viano, D.C., Melvin, J.W., McCleary, J.D., Madeira, R.G., Shee, T.R., and Horsch, J.D., *Measurement of Head Dynamics and Facial Contact Forces in the Hybrid III Dummy*, Proceedings of the Thirtieth Stapp Car Crash Conference, Society of Automotive Engineers, Warrendale, PA, 1986.

APPENDIX A

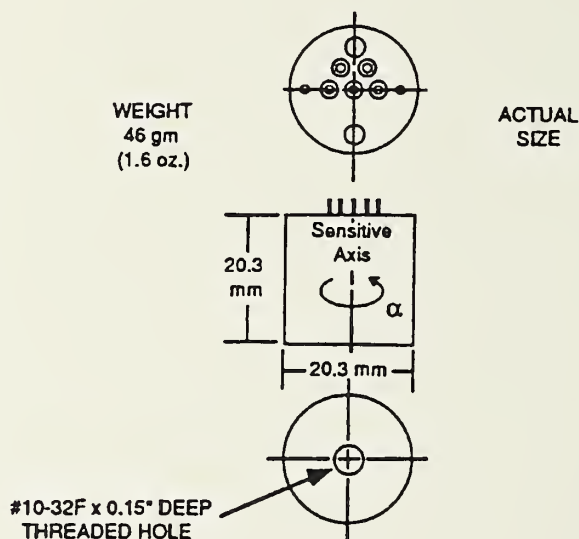
ATA

applied

technology associates, inc.

1900 Randolph, SE, Albuquerque, NM 87106
(505) 247-8371, FAX (505) 768-1379

[Preliminary] MHD ANGULAR ACCELERATION SENSOR MODEL AAS-01



FEATURES:

- No mechanical moving parts
- Dynamic range exceeding 100 dB
- Hermetically sealed unit
- High g survivability
- Low power consumption
- Low cross axis angular and linear acceleration sensitivity
- Inertial angular rate measurement over more than three frequency decades
- Relatively low mass and volume for comparable performance angular sensors
- Integral thick film hybrid electronics for maximum signal-to-noise ratio

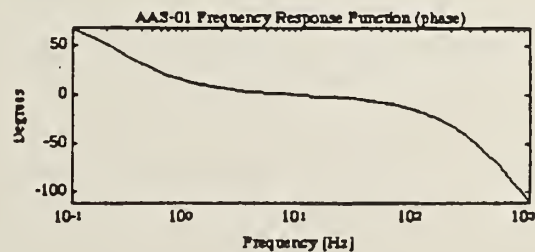
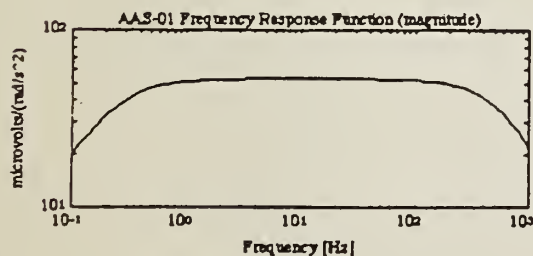
MODEL AAS-01 SPECIFICATIONS

SPECIFICATION	UNIT	RANGE
DYNAMIC:		
Range (1):	rad/s ² (deg/s ²)	$\pm 6.3 \times 10^4$ ($\pm 3.6 \times 10^4$)
Sensitivity (@100 Hz):	$\mu\text{v}/\text{rad/s}^2$ ($\mu\text{v}/\text{deg/s}^2$)	50 (0.87)
Bandwidth (-3 dB points):	Hertz	0.3- 500
Cross Axis Angular Error:	%	< 2
Linear Acceleration Sensitivity (2):	Eq. (rad/s ²)/g ((deg/s ²)/g)	< 1 (60)
Angular Acceleration Noise PSD (3):	Eq. (rad/s ²) ^{1/2} /Hz ((deg/s ²) ^{1/2} /Hz)	1×10^{-4} F (3.3×10^{-3} F)
Non-Linearity:	%	< 1
Temperature Coefficient (4):	% SF/°C	< 0.05
ELECTRICAL:		
Excitation:	Vdc	± 5 to ± 15
Power Dissipation:	watts	< 0.3
Output Impedance:	Ω	~ 250
Grounding: (see note 5)		
PHYSICAL:		
Weight:	grams (oz)	46 (1.6)
Diameter:	mm (in)	20.3 (0.80)
Height:	mm (in)	20.3 (0.80)
Mounting Torque:	Nm (in lb)	2 (18)
ENVIRONMENTAL:		
Maximum Linear Acceleration (6):		
Operational (All Axes):	g	1,000
Survivable (All Axes):	g	3,000
Temperature Range:		
Operational:	°C (°F)	-30 to 50 (-22 to 122)
Survivable:	°C (°F)	-60 to 100 (-76 to 212)

Notes:

1. Peak-to-peak sine at 100 Hz with ± 15 Vdc excitation
2. Measured @ 10 Hz
3. f is in Hz
4. Percent change in scale factor (SF) @ 100 Hz per °C
5. Signal return connected to case (insulated mounting stud provided)
6. Peak, 100 Hz half sine

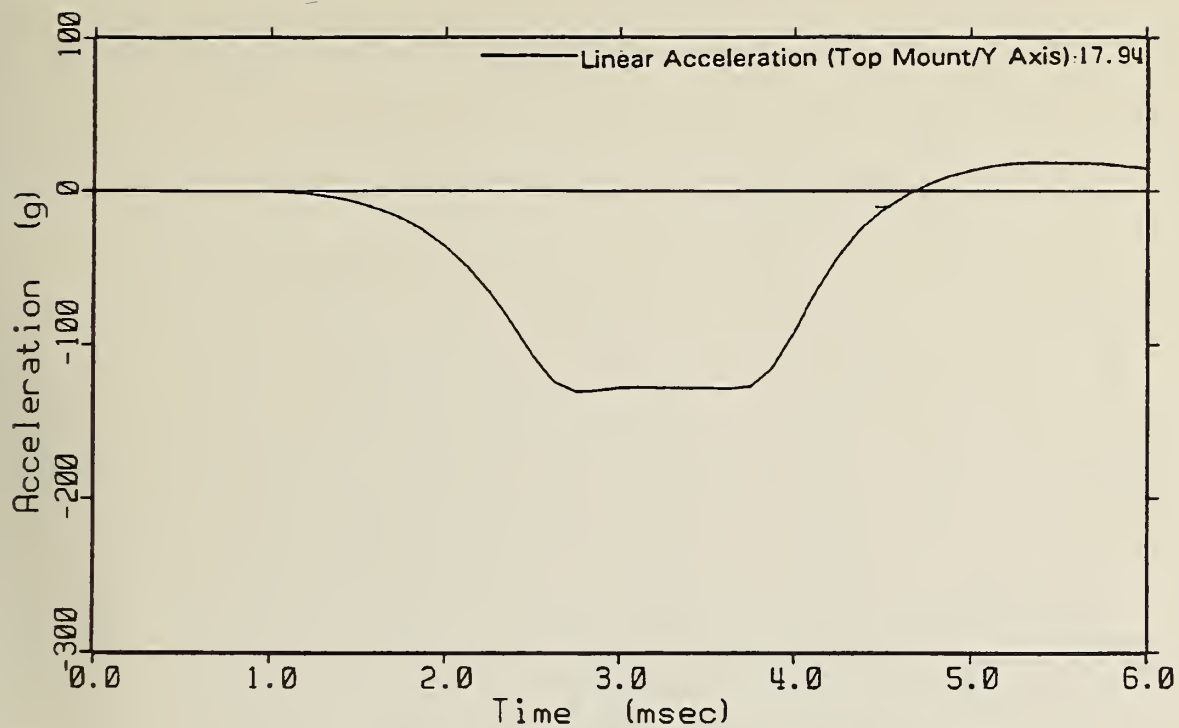
TYPICAL FREQUENCY RESPONSE



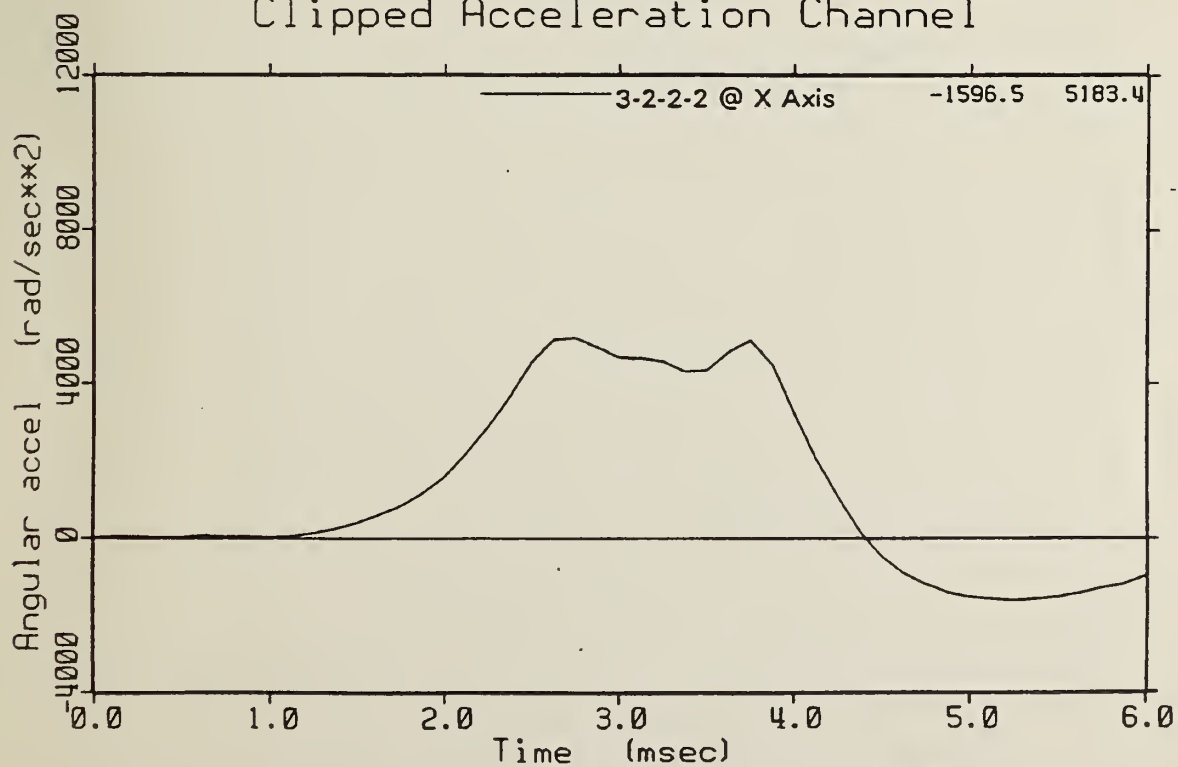
Reference 91M0022

Applied Technology Associates, Inc.
1900 Randolph Road, SE
Albuquerque, New Mexico 87106
TEL: (505) 247-8371 FAX: (505) 768-1379

APPENDIX B



Clipped Acceleration Channel



Calculated Angular Acceleration @ X Axis

Figure B1 - Clipped Channel (Test 02260058)

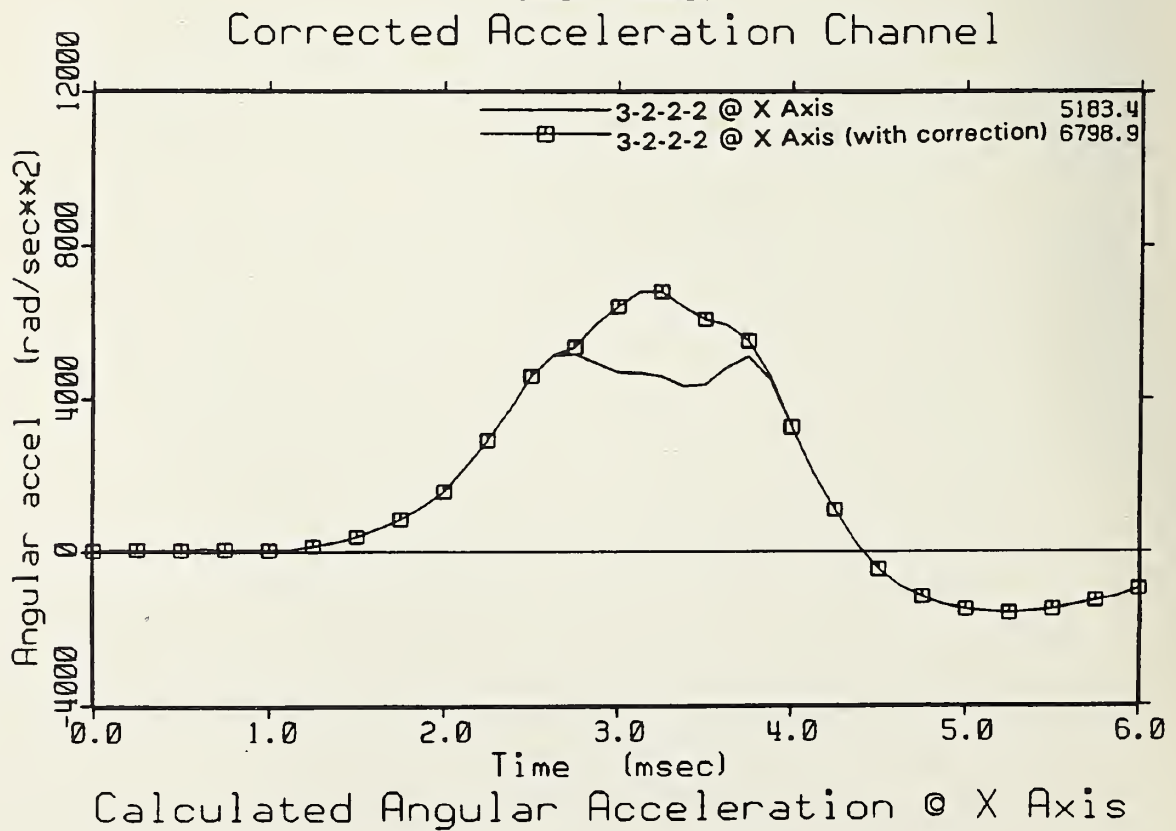
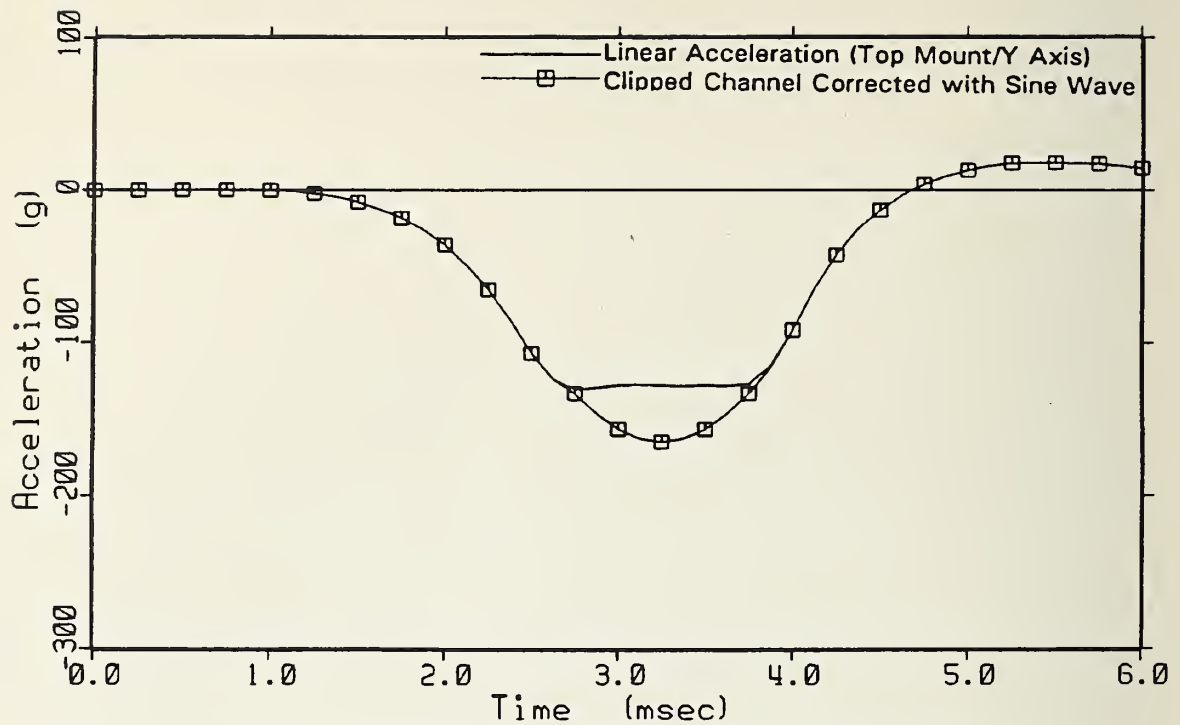


Figure B2 -- Corrected Channel

DOT LIBRARY



00302573